Trophic ecology of the squid Doryteuthis gahi in the Southwest Atlantic inferred from stable isotope analysis

Tobias Büring, Jessica B Jones, Graham J Pierce, Francisco Rocha, Paco Bustamante, Maud Brault-Favrou, Alexander Arkhipkin

Trophic ecology of the squid *Doryteuthis gahi* in the Southwest Atlantic inferred from stable isotope analysis

Tobias Büring*[,1,4], Jessica B. Jones[2], Graham J. Pierce[3], Francisco Rocha[4], Paco Bustamante[5,6], Maud Brault-Favrou[5], Alexander I Arkhipkin[1]

[1]*Falkland Islands Fisheries Department*

[2]*Scottish East Coast Review (SEaCoR), Forth Estuary Forum, Scotland*

[3]*Instituto de Investigacións Mariñas*

[4]*Universidade de Vigo, Departamento de Ecología y Biología Animal, Campus de Vigo As Lagoas-Marcosende, 36310 Vigo, Spain*

[5]*LIttoral, Environnement and Societés (LIENSs), UMR 7266 CNRS – La Rochelle Université, 17000 La Rochelle, France*

[6] *Institut Universitaire de France (IUF), 1 rue Descartes 75005 Paris, France*

**Corresponding Author*

Abstract: The Patagonian longfin squid *Doryteuthis gahi* has an annual life cycle with two seasonal cohorts (autumn and spring spawners). Previous studies estimated the trophic level of adult squid by stable isotope analysis of their muscle or gladius tissues, but few studies compared different sizes and spawning cohorts. In this study, mixed models were used to compare carbon ($\delta^{13}C$) and nitrogen ($\delta^{15}N$) stable isotope signatures of muscle and gladius tissues of the autumn and spring spawning cohorts and squid of different sizes. A published isoscape model provided $\delta^{15}N$ baselines to calculate the trophic level of *D. gahi*. Sampled herbivorous prey such as Euphausiacea, planktonic juveniles *Munida gregaria* and salps *Ihlea* supported the trophic level estimates. The autumn spawning cohort had higher $\delta^{13}C$ values than the spring spawning cohort. $\delta^{15}N$ values increased with increasing dorsal mantle length, suggesting an ontogenetic change towards larger prey. Muscle tissue was enriched in ^{15}N but slightly depleted in ^{13}C compared to gladius tissue. Adult squid had an estimated trophic level of ~3.2, with no significant differences between spawning cohorts. Stable isotope values followed a seasonal trend, with lower $\delta^{15}N$ values and lower $\delta^{13}C$ value between July and September. Large individuals of the spring spawning cohort were found to have the least niche overlap with other groups of *D. gahi*. Our study of the trophic levels and ecology of *D. gahi* can provide important information on its role in the food chain and can build the basis of studies on interaction with other species, and the impact of environmental changes on their populations. This information can inform the development of management strategies aimed at preserving the balance of the ecosystem and ensuring its sustainable use.

Keywords: Stable isotopes; Trophic niche; Spawning cohorts; Patagonian shelf; Squid

1. Introduction

Squid are one of the main components of marine food webs linking primary consumers and marine top predators (Coll et al., 2013; Gasalla et al., 2010; Navarro et al., 2013). They are active predators with their diet ranging from small zooplankton to cephalopods and fish (Guerra et al., 1991; Markaida and Sosa-Nishizaki, 2003; Pierce et al., 1994; Rodhouse and Nigmatullin, 1996). Identification of prey items in stomach contents of squid is difficult as squid macerate their food before ingestion and in some cases might reject identifiable parts such as fish heads (Porteiro et al., 1995), complicating classical stomach content analysis (Boyle and Rodhouse, 2005). As a result, alternative methods such as serological analysis (Boyle and Rodhouse, 2005; Grisley and Boyle, 1985, 1988) or stable isotope analysis (SIA) have been used to support stomach content analysis to determine the diet and trophic levels of squid (Navarro et al., 2013; Ruiz-Cooley et al., 2004, 2006). Specifically, nitrogen ($^{15}N/^{14}N$) and carbon ($^{13}C/^{12}C$) ratios denoted as δ, can be used to study the ecotrophic niche of a species (Bearhop et al., 2004). Carbon isotope ratios change relatively little per trophic level in marine ecosystems, on average between 0.4 and 1.3 ‰ (McCutchan et al., 2003). Different sources of carbon fixation in primary producers can lead to larger differences in $\delta^{13}C$ within the ecosystem (Fry, 2006), and it is thus essential to know the "baseline" carbon isotope ratio. The main differences in $\delta^{13}C$ have been found between coastal and offshore waters, with the latter normally being more depleted in ^{13}C (France, 1995; Miller et al., 2008), between benthic and pelagic ecosystems due to different food carbon sources (Fry, 2006) and between lower and higher latitudes (Jaeger et al., 2010). A retention of the heavier nitrogen isotope (^{15}N) in biological processes compared to the lighter form (^{14}N) leads to an average enrichment of around 3.4 ‰ $\delta^{15}N$ per trophic level (Minagawa and Wada, 1984), although higher trophic levels might experience greater variations (Ruiz-Cooley et al., 2021). As the range of $\delta^{15}N$ values in seawater can vary between 0 and 12 ‰ (i.e., higher than the enrichment factor per

trophic level; Somes et al., 2010), it is also necessary to adjust the estimate of the trophic level based on the $\delta^{15}N$ values in primary producers or consumers (Cabana and Rasmussen, 1996; Navarro et al., 2013). Instead of taking the of $\delta^{15}N$ values in primary producers in their region into account, some studies have relied upon literature values to estimate trophic level of primary producers, which could lead to unreliable estimates (Rosas-Luis et al., 2017). Furthermore, the use of SIA does not allow to identify single prey species and is dependent on mixing models including reference species from the same area (Phillips et al., 2014), which makes it advisable to use a combination of SIA and classical stomach content analysis.

Within an organism, each tissue type has a different rate of turnover. Muscle and liver tissue have a turnover rate of days to weeks, whereas hard structures such as calcified tissues metabolise much slower and therefore have a lower turnover rate of months to years (Sweeting et al., 2005). The trophic position of a species can therefore be studied over a longer time period by using SIA compared to stomach content analysis, which reflects the diet just prior to capture (Post, 2002; Rosas-luis et al., 2016). In squid, the gladius can be used to study the species diet over a longer time span, but the youngest piece (anterior end) of the gladius can give information about the recent trophic level of the squid (Rosas-Luis et al., 2017; Ruiz-Cooley et al., 2010).

The Patagonian longfin squid *Doryteuthis gahi* (Loliginidae) is an abundant medium-sized squid distributed along the Patagonian Shelf of the Southwest Atlantic and in the Southeast Pacific (Jereb and Roper, 2010). The population structure of *D. gahi* in Falkland Islands waters consists of two main annual cohorts characterized by different seasons of spawning – the autumn-spawning cohort (ASC) and the spring-spawning cohort (SSC). Hence, the same ontogenetic phases of squid from each cohort lives in different seasons and in different habitats, experiencing different environmental conditions, such as different temperature regimes and depth distributions (Arkhipkin et al., 2004; Jones et al., 2018). These environmental conditions

also apply to the prey species of *D. gahi* and therefore the diet differs between the two cohorts (Büring et al., 2022).

D. gahi is an active predator, feeding on planktonic crustaceans, chaetognaths, fish and squid (Büring et al., 2022; Guerra et al., 1991; Rosas-Luis et al., 2014). The most important prey species throughout the whole lifecycle of *D. gahi* are Euphausiacea, such as *Euphausia lucens* (Büring et al., 2022; Guerra et al., 1991; Rosas-Luis et al., 2014). *E. lucens* is typically herbivorous but can also switch to a diet consisting of copepods when the concentration of algae decreases (Gibbons et al., 1991). Another important prey species of *D. gahi* is the planktonic stages of the lobster krill *Munida gregaria* (Brickle et al., 2002; Büring et al., 2022). Previous studies found $\delta^{15}N$ values in the gladius of *D. gahi* ranged from 6 to 12 ‰ and $\delta^{13}C$ values between -23 ‰ and -19 ‰, which were comparable with isotopic values of *Illex argentinus* (Rosas-Luis et al., 2016, 2017). According to Rosas-Luis et al. (2016) the trophic level of *D. gahi* was estimated based on *Salpa thompsoni* values (Perissinotto and Pakhomov, 1998), resulting in an unrealistic trophic level of ~5. This is higher than the trophic levels of much larger squid species, such as the giant squid *Architeuthis dux* (trophic level 4.6) and the colossal squid *Mesonychoteuthis hamiltoni* (trophic level 6.1) (Cherel et al., 2008; Guerreiro et al., 2015). However, the studies by Rosas-Luis et al. (2016, 2017) were based on limited samples and a lack of baseline information,

making it impossible to conduct a comprehensive analysis of ontogeny

or comparisons between spawning cohorts.

The present study aims to investigate the trophic niche of different size groups of both cohorts of *D. gahi* by analysing $\delta^{13}C$ and $\delta^{15}N$ values of muscle tissue for a short-term signal and the anterior end of the gladius for a medium-term signal based on recent nitrogen baseline values. Furthermore, we compared muscle with gladius tissues and modelled the relationship between the tissue types. The aim is to differentiate between the trophic niches and trophic levels of the

two spawning cohorts of *D. gahi* and to gain deeper insights into differences of their feeding ecology.

2. Material and Methods

2.1. Sample collection and processing

D. gahi specimens (n = 269) were collected throughout 2020 in waters around the Falkland Islands as well as from international waters at latitude 45°S aboard bottom trawling fishing vessels and during two research cruises, which used also bottom trawling gear (Fig. 1). In addition, zooplankton samples were collected at three stations during the research cruises and onboard a small vessel near Stanley Harbour (see section 'Zooplankton samples').

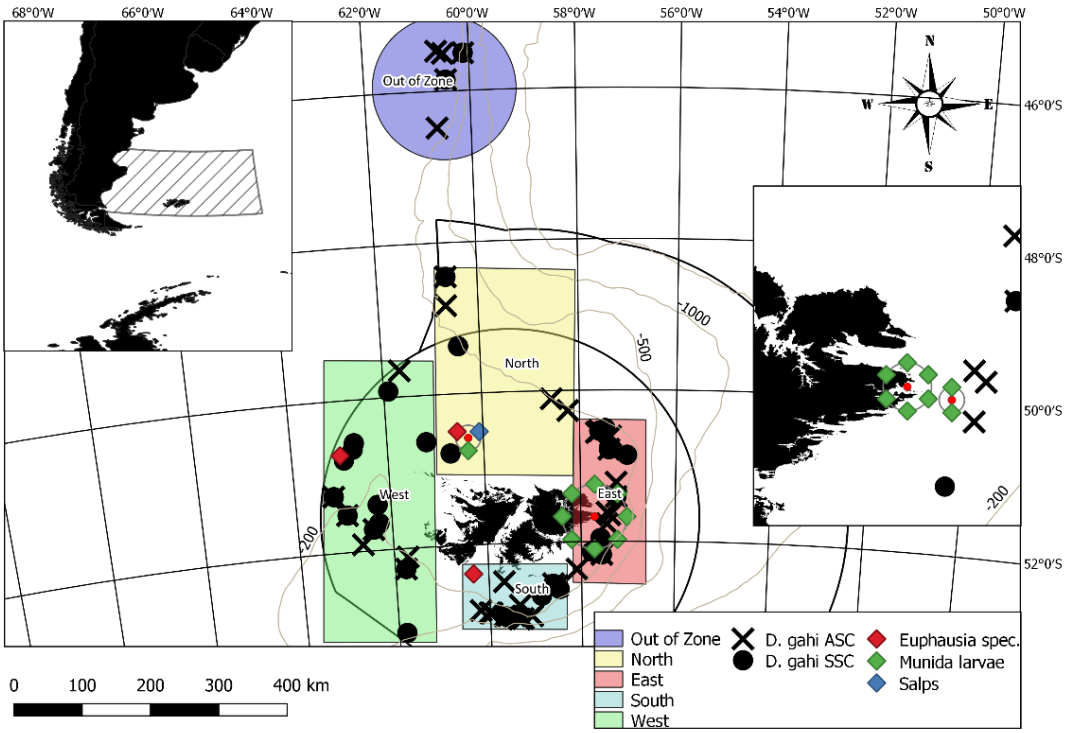

Figure 1. Overview map (top left) and sampling area of *Doryteuthis gahi* samples (autumn spawning (ASC) and spring spawning cohort (SSC)) and zooplankton samples around the Falkland Islands, with Falkland Islands inner (FICZ) and outer (FOCZ) conservation zones; sampling areas shaded.

The depth range of sampling stations for *D. gahi* was 100–400 m with a median of 170 m. The mean sampling depth of the ASC was 165 m, while the mean sampling depth of the SSC was 199 m. Samples were divided into five areas: North (<52° South), East (<58° West), South (>52° South), West (>61° West) and High Seas (North of the FICZ; the spatial distribution of samples is addressed in the statistics section). Areas accounting for the different current regimes, such as the South and East are influenced by the Falkland/Malvinas Current, whereas West, North and 'Out of Zone' are influenced by the Argentine drift (Acha et al., 2004; Thorpe, 2009). Further subdivisions were made to account for stock assessment models of *D. gahi* from the Fisheries Department (Winter, 2021a, 2021b). Individuals were frozen and brought to the Falkland Islands Fisheries Department laboratory for further analysis.

Once defrosted, dorsal mantle length (DML ±0.5 cm) and total body mass (TW ±0.1 g) were measured and individuals were visually assessed for sex and maturity stages 1–5 (Lipinski, 1979, Table 1). The individuals for the study were selected from random samples of 100 individuals, with the aim to collect equal amounts of each size class, sex and from various regions throughout the year. Therefore, 2 small, 2 medium and 2 large individuals belonging to each sex were taken if available. Individuals were assigned to each spawning cohort using their DML, maturity and month of collection. For individuals sampled in February, the depth in which they were caught was also taken into account (large ASC individuals occur in deeper waters, whereas small immature SSC individuals occur in shallower waters), based on findings by Arkhipkin et al. (2004; 2013).

A 1 cm² piece of muscle tissue was dissected from the mantle at the dorsal anterior part of the body (Fig. 2). The skin was removed, the tissue was flushed with distilled water and stored dry in an Eppendorf tube. For the gladius, a subsample from the whole sample (n = 124) was taken, which was chosen to ensure a range of DML and that both sexes were included. These samples were cleaned with distilled water, measured for total gladius length (±0.1 cm) and then cut into 5 pieces of equal length from the posterior part (i.e., the oldest material representing the juvenile stage) to the anterior part (i.e., the youngest material representing the adult stage (Arkhipkin et al., 2012); and the wing sections were removed (Fig. 2).

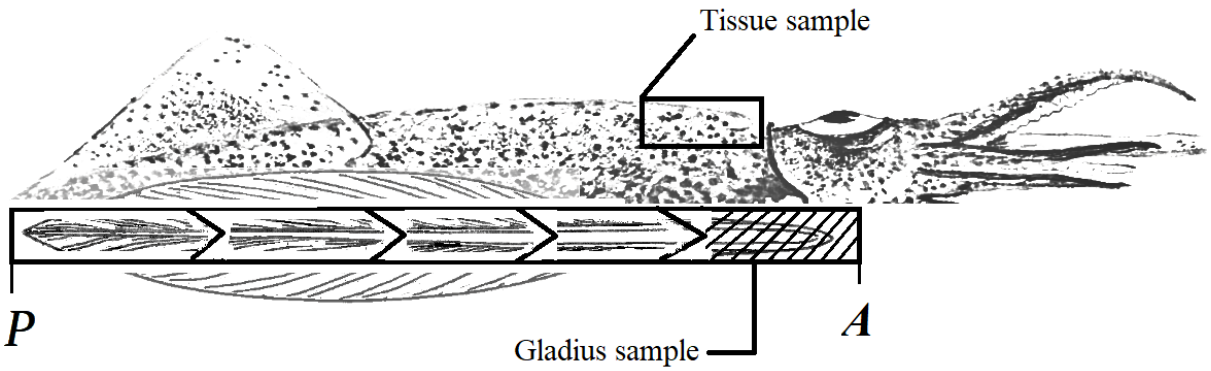

Figure 2. Schematic view of *Doryteuthis gahi* with position of the gladius. P = Posterior part (oldest part representing juvenile stage), A = Anterior part (youngest part representing adult stage); locations of the tissue sample and the gladius sample are included.

Only the anterior part of the gladius was used for further analysis. To follow the direction of the growth increments, sections were cut in a Vshape (Lorrain et al., 2011) and stored dry in Eppendorf tubes.

Table 1. Number of individuals sampled, mean DML in cm and standard deviation per tissue type summarised by spawning cohorts (autumn spawning (ASC) and spring spawning cohort (SSC)) and sex (males and females); *gladius tissue was taken from the same individuals which were sampled for muscle tissue

Type	Cohort	Sex	Length	n*
Gladius	ASC	F	10.63 ± 2.54	34
		M	13.35 ± 6.38	37
	SSC	F	10.97 ± 3.53	25
		M	15.15 ± 6.85	28
Muscle	ASC	F	11.07 ± 3.09	78
		M	13.10 ± 5.75	79
	SSC	F	11.32 ± 3.86	49
		M	14.54 ± 6.48	63

2.2. Zooplankton samples

To allow for comparisons of $\delta^{15}N$ values from this study with other ecosystems and studies, and to incorporate seasonal and spatial variability in the $\delta^{15}N$ of small organisms responsible for the ecosystem N baseline in the year of sampling 2020, the approach by Cabana and Rasmussen (1996) was followed.

1. Larval and early juvenile planktonic *Munida gregaria* were collected out of zooplankton samples taken on board the PV Protegat during February 2020 with a 500 µm mesh size Bongo net from depths between 50 and 200 m and a tow time of approximately 30 min.

2. *M. gregaria* planktonic juveniles were sampled onboard the SAERI (South Atlantic Environmental Research Institute) RV Jack Sollis near Stanley Harbour with a 350 µm mesh Bongo net during February, September and November 2020 in a depth of around 5 m with a tow time of 10 min.

3. In February and June 2020, salps of the genus *Ihlea*, Euphausiacea, Chaetognatha and Amphipoda were collected on board the FV Castelo with a 500 µm Isaacs-Kidd plankton net by horizontal trawling (20–150 m depth). Single plankton species were identified using an identification key (Boltovskoy, 1999), but salps could not be identified to species level due to the sample condition (damaged).

Individuals of each species were pooled and species were stored separately to obtain average $\delta^{15}N$ baseline data from the ecosystem of the Falkland Islands.

2.3. Stable isotope measurements

Zooplankton samples, muscle tissue and gladius fragments of *D. gahi* were oven dried for 24 h at 80 °C. Samples were then ground into a fine homogenous powder with a porcelain pestle and mortar prior to sending them to LIttoral, ENvironnement and Societ´es (LIENSs) Joint Research Unit stable isotope facility (CNRS – La Rochelle Université, France) for further processing. Each sample was then weighed into a tin container using a Sartorius M5 microbalance (±1 µg). The ratios of the heavier ^{13}C and ^{15}N to the lighter ^{12}C and ^{14}N, respectively, as well as the C/N ratio were measured using a Flash 2000 elemental analyser (Thermo Scientific, Milan, Italy) coupled with a Delta V Plus isotope ratio mass spectrometer with a Conflo IV interface (Thermo Scientific, Bremen, Germany). Results are expressed in the δ unit notation as per mil (‰) deviation from the international standards Vienna-Pee Dee Belemnite ($\delta^{13}C$) and atmospheric N_2 ($\delta^{15}N$). Isotope values are reported as $\delta^{13}C$ or $\delta^{15}N$ values:

$$\delta R_{sample} = [(R_{sample}/R_{standard}) - 1] \times 10^3 \ (eq. 1)$$

where R is $^{13}C/^{12}C$ or $^{15}N/^{14}N$, respectively.

The analytical precision was ±0.10 ‰ for $\delta^{13}C$ and ±0.15 ‰ $\delta^{15}N$ based on internal standards USGS-61 and USGS-62 inserted every ten measurements.

The trophic level was calculated with two methods:

1. With the equation provided by different studies (Cabana and Rasmussen, 1996; Stowasser et al., 2012; Sweeting et al., 2005) trophic level was calculated using the formula:

$$TL_{consumer} = [(\delta^{15}N_{consumer} - \delta^{15}N_{\substack{primary \\ consumer}})/3.4] + 2 \quad (eq.\,2a)$$

Where 3.4 represents an average enrichment in ^{15}N per trophic level (Minagawa and Wada, 1984) and 2 is the reference value for trophic position 2 (Cabana and Rasmussen, 1996; McCutchan et al., 2003; Montecinos et al., 2016; Stowasser et al., 2012).

2. We used the isoscape data provided by St John Glew et al. (2021), where a δ^{15}N baseline was modelled in R-INLA (integrated nested Laplace approximation) for the Southern Ocean, originally based on POM (particulate organic matter) measurements. Data was extracted from their first interaction model for each season and location of our samples and applied to our samples. With the modified eq. 2

$$TL_{consumer} = [(\delta^{15}N_{consumer} - \delta^{15}N_{\substack{primary \\ consumer}})/3.4] + 1 \quad (eq.\,2b)$$

where 1 represents trophic level 1 of POM, trophic levels were calculated for each sample. The isoscape model was subdivided into seasons: Jan-Feb, Mar-Apr, May-Oct and Nov-Dec, so we assigned our samples accordingly.

To find the relationship between gladius and muscle δ^{15}N values, a linear model was fitted to a subset of the data (n = 124), in which gladius and muscle tissue were measured for the same individual.

2.4. Statistical analysis

2.4.1. Generalized additive mixed effect models

All calculations, statistics and plots were made using R.4.03 (R Core Team 2020). Generalized additive mixed effect models (GAMMs) were used in this study firstly because GAMs and GAMMs permit the inclusion of non-linear relationships (Hastie and Tibshirani, 1986), such as cyclicity over the year, and secondly to account for the spatial structure of the data (Zuur et al., 2009). To account for spatial patterns, samples were divided into five sampling areas. This 5-factor variable was incorporated as a random effect in the GAMMs. Maturity stages were pooled into 1-3 as immature/maturing and 4-5 as mature. We fitted Gaussian models (with an identity link function), which appeared to be reasonable for the SI data. Models with all possible combinations of explanatory variables such as DML (continuous), day (continuous; representing day of the year ranging from 1 to 365), maturity (two level factor) and sex (two level factor) and including all biologically relevant two-way interactions between effects of all pairs of explanatory variables were compared based on their Akaike Information Criterion (AIC). Four separate GAMMs (eq. 5a to 5d) with a Gaussian distribution and an identity link were chosen to investigate the relationship between stable isotope values (C and N) for each tissue type (muscle and gladius), day of the year on which the squid were sampled and DML of the squid.

$$gamm(\delta^{15}N_{muscle} \sim s(DML) + s(Day, bs = \text{cc}), random = list(Area = \sim 1))(eq.\,3a)$$

$$gamm(\delta^{15}N_{gladius} \sim ti\big(DML, Day, bs = (\text{cs}, \text{cc})\big) + s(DML) + s(Day, bs = \text{cc}), random = list(Area = \sim 1))(eq.\,3b)$$

$$gamm(\delta^{13}C_{muscle} \sim ti\big(DML, Day, bs = (\text{cs}, \text{cc})\big) + s(DML) + s(Day, bs = \text{cc}),$$
$$random = list(Area = \sim 1))(eq.3c)$$

$$gamm(\delta^{13}C_{gladius} \sim ti\big(DML, Day, bs = (\text{cs}, \text{cc})\big) + s(DML) + s(Day, bs = \text{cc}),$$
$$random = list(Area = \sim 1))(eq.3d)$$

where *s()* describes a smoothing term for a continuous variable; *ti()* describes an interaction between two continuous variables in form of a tensor; *bs* = represents the regression cubic splines in which 'cc' stand for cyclic cubic splines, whereas 'cs' are cubic splines which represent knots spread evenly through the covariate values; random = represents the random effect of the model, in this case ~Area (the list attribute is used for coding).

The smoother day of the year was chosen, as it represents the seasonal occurrence of the two spawning cohorts. For each combination of C and N of muscle and gladius tissue (4 combinations), the model with the lowest AIC was chosen, removing non-significant co-variates and interactions. The significance of the interaction between the two continuous explanatory variables was quantified using a tensor rather than a 'three-dimensional smoother'. We used a tensor, because it permits separate evaluation of the significance of the interaction and because of the cyclicity of the factor day of the year (day 1 follows day 365) and tensors can be used with cyclic cubic splines, i.e. penalised cubic regression splines whose ends meet up. We used the *ti()* function rather than the *te()* function from the R package 'mgcv', as *ti()* is appropriate when the main effects are to be included separately from the tensor product interaction (Wood, 2017; Zuur et al., 2009). If the interaction was determined as significant, for visualisation purposes, we reran the models, using the *te()* function. The *te()* function incorporates the main effects, also then deleting the separate terms for the two main effects, allowing us to visualise the combined effect of DML and day of year – this is technically still the same model.

Another simpler GAM was used to analyse the effect of seasonality on trophic levels assigned with isoscapes of both tissue types, using day of the year as continuous variable, 'Tissue' as a 2 level factor and a cyclic cubic spline:

$$gam(TL \sim s(Day, by = Tissue, bs = \text{cc}) \ (eq. 4)$$

All GAM(M)s were performed using the R package 'mgcv' (Wood, 2017). Plots were made using the R package 'ggplot2' (Wickham, 2016).

2.4.2. Trophic niche

Data were split into two spawning cohort groups, for individuals belonging to the ASC and SSC and into three size-classes (small ≤8 cm; medium = 8-19 cm; large = ≥20 cm) to make inter-seasonal comparisons as in Büring et al. (2022). These groups (spawning cohorts and size groups) were used to estimate trophic levels and trophic niches, following a Bayesian multivariate model approach, performed using the R package 'SIBER' v.2.1.6 (Jackson et al., 2011) and 'nicheROVER' (Lysy et al., 2021). Number of Monte Carlo draws (iterations) was set to 1000 and alpha to 95%. Trophic niche in this context is referring to the SI niche when analysing $\delta^{13}C$ and $\delta^{15}N$ values together (Bearhop et al., 2004).

3. Results

For $N_{Gladius}$, C_{Muscle} and $C_{Gladius}$ (eq. 3b to 3d) an interaction between DML and day of the year was found to improve model fit (AIC; Table S1 supplementary material). Day of the year and DML were the most important co-variates for both muscle and gladius carbon and nitrogen signatures (4 separate models; eq. 3a to 3d), whereas sex and maturity did not improve the model fit. $\delta^{15}N$ values of muscle tissue were significantly affected by DML and day of the year (GAMM, Table 2), but an interaction between these co-variates did not seem to improve model

fit, with an AIC of 667 vs an AIC of 664 in (Table S1, supplementary material), therefore the simplest model specification eq. 3a was chosen.

3.1. $\delta^{15}N$ values

3.1.1. Muscle tissue

$\delta^{15}N$ values increased towards austral winter months (Jun-Aug) and were the lowest during austral summer months (Nov-Feb) and increased with increasing DML (Fig. 3). The effects of day of the year and DML were both significant ($p<0.001$, GAMM smoother, Table 2), even though deviance explained by the model was only 8%. P-values of GAMs and GAMMs are only approximate and should be interpreted with care (Zuur et al., 2009).

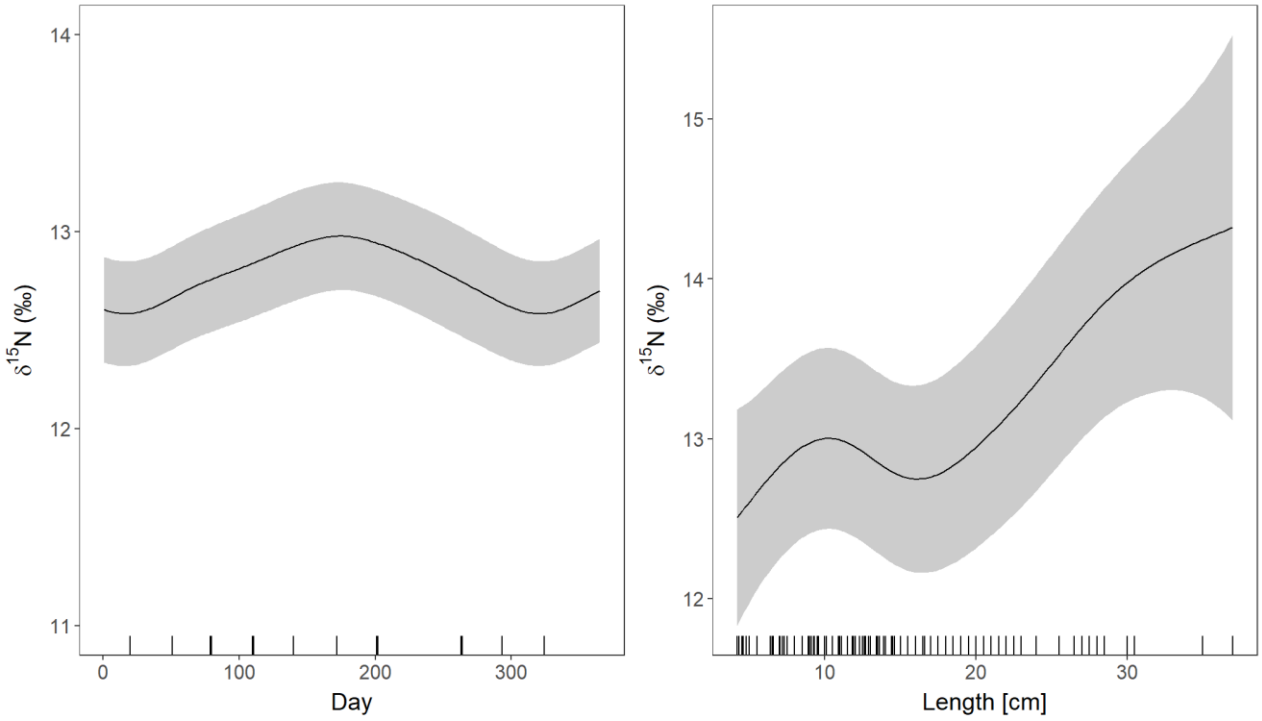

Figure 3. Estimated smoothing curves from the GAMM for $\delta^{15}N$ values of muscle tissue vs. DML [cm] and day of the year; grey shaded area representing 95% confidence interval

Table 2. Overall model performance (R-sq.) and smoothers of the fixed effects of the GAMMs for $\delta^{15}N$ and $\delta^{13}C$ for each tissue type muscle and gladius; edf = expected degrees of freedom, F value and p-value

Isotope	Tissue	Model	R-sq.(adj)	smoother	edf	F	p-value
$\delta^{15}N$	Muscle	Eq. 3a	0.08	s(DML)	4.2	6.44	<0.001
				s(Day)	2.1	1.16	0.005
	Gladius	Eq. 3b	0.30	ti(DML,Day)	3.1	1.47	<0.001
				s(DML)	4.5	5.00	0.003
				s(Day)	2.4	3.39	<0.001
$\delta^{13}C$	Muscle	Eq. 3c	0.51	ti(DML,Day)	5.4	4.17	<0.001
				s(DML)	1.0	6.50	0.011
				s(Day)	6.3	31.12	<0.001
	Gladius	Eq. 3d	0.78	ti(DML,Day)	5.4	3.48	<0.001
				s(DML)	5.1	4.14	0.002
				s(Day)	4.7	20.02	<0.001

3.1.2. Gladius tissue

Like muscle tissue, $\delta^{15}N$ values in gladius tissue were significantly affected by DML and day of the year, explaining 30% of the deviance (Table 2). In gladius tissue, a pronounced positive trend of increasing $\delta^{15}N$ values with DML could be observed (Fig. 4B) and the interaction of DML with day of the year was found to be significant (Table 2, Fig. 4C).

We reran the model with the *te()* smoother to account for the significant interaction.

$$gamm(\delta^{15}N_{gladius} \sim te\big(DML, Day, bs = (\text{cs}, \text{cc})\big),$$

$$random = list(Area = \sim 1))(eq.5a)$$

According to the model (eq. 5a), small ASC individuals in February had higher $\delta^{15}N$ values compared to small SSC individuals in September (Fig. 4D). Large individuals of the ASC

(found in July-August) had higher $\delta^{15}N$ values later on in the year compared to large SSC individuals (found in December - January).

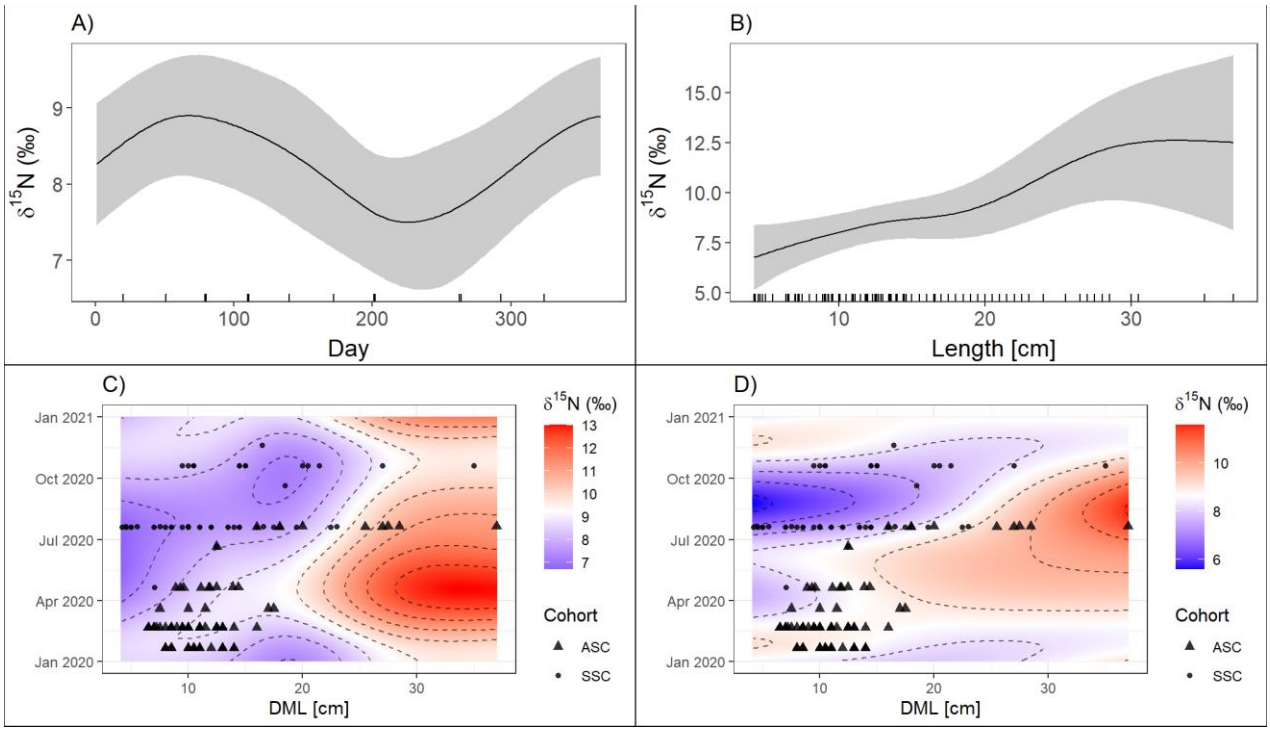

Figure 4. Estimated smoothing curves from the GAMM for $\delta^{15}N$ values of gladius tissue vs. A) DML [cm] and B) day of the year; C): ti-tensor (interaction excluding main effects) of day of the year and DML [cm]; D): te-tensor (interaction including main effects) of day of the year and DML [cm]; triangles = ASC, circles = SSC

3.2. $\delta^{13}C$ values

3.2.1. Muscle tissue

Similar to the model testing N of muscle tissue, the GAMM revealed that $\delta^{13}C$ values in muscle tissue were influenced by DML and day of the year (Table 2), explaining 52% of the deviance. $\delta^{13}C$ values were the lowest in Sep-Nov (austral spring), highest in Feb-Mar (austral autumn), and steadily increased with increasing DML. The interaction between DML and day of the year

was very pronounced (p<0.001, GAMM, Table 2, Fig. 5C), therefore we reran the model (eq. 5b).

$$gamm(\delta^{13}C_{muscle} \sim te(DML, Day, bs = (\text{cs}, \text{cc})),$$
$$random = list(Area = \sim 1))(eq.5b)$$

Small individuals (~10 cm) of the ASC in February had higher δ^{13}C values (~-18 ‰) compared to small SSC individuals around September (~-20 ‰; Fig. 5D).

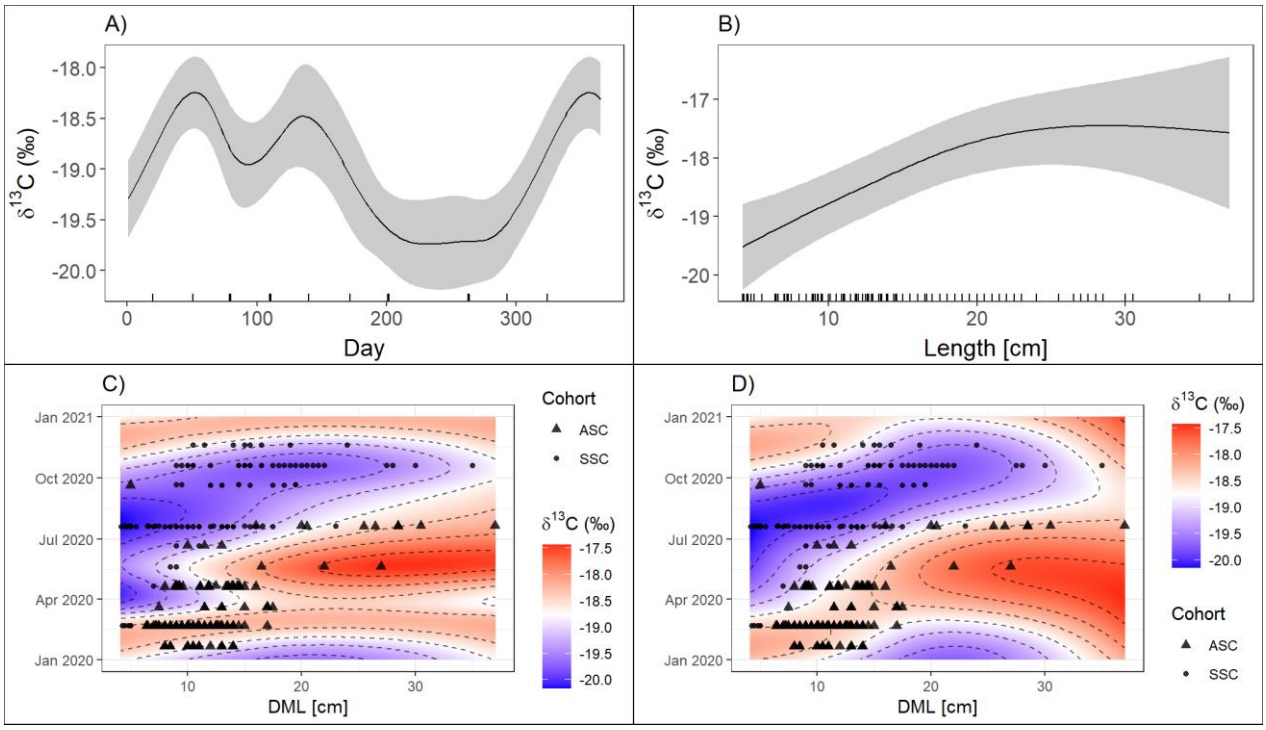

Figure 5. Estimated smoothing curves from the GAMM for δ^{13}C values of muscle tissue vs. A) DML [cm] and B) day of the year; C): ti-tensor (interaction excluding main effects) of day of the year and DML [cm]; D): te-tensor (interaction including main effects) of day of the year and DML [cm]; triangles = ASC, circles = SSC.

Large individuals (~20 – 30 cm DML) of both cohorts were found to have higher $\delta^{13}C$ values in the latter part of the year (Fig. 5D). The highest $\delta^{13}C$ values of approximately -17 ‰ $\delta^{13}C$ could be found in May in individuals ~30 cm DML.

3.2.2. Gladius tissue

The $\delta^{13}C$ values of gladius tissue were significantly influenced by DML and day of the year ($p<0.001$, GAMM, Table 2). The trends observed in the model were similar to $\delta^{13}C$ values of muscle tissue. In contrast to muscle tissue, the $\delta^{13}C$ values in the gladius did not follow a certain trend with increasing DML (Fig. 6B), but a strong interaction between DML and day of the year ($p<0.001$, Table 2) was found (Fig. 6C). Therefore, the model was reran with the *te()* function (eq. 5c).

$$gamm(\delta^{13}C_{gladius} \sim te(DML, Day, bs = (\text{cs, cc})),$$
$$random = list(Area = \sim 1))(eq.5c)$$

Individuals belonging to the ASC, found mainly during February to May, had higher $\delta^{13}C$ values (~-18 to -17 ‰) compared to SSC individuals found between June and December (~-20 to -18 ‰, Fig. 6D).

3.3. Zooplankton $\delta^{15}N$ and $\delta^{13}C$ values

Euphausiacea, salps and larval *M. gregaria* were assumed to rank between primary and secondary consumers (Castro et al., 2021; Gibbons et al., 1991; Perissinotto and Pakhomov, 1998). Values of $\delta^{15}N$ of *M. gregaria* ranged from 7.64 to 11.45 ‰ (Table 3).

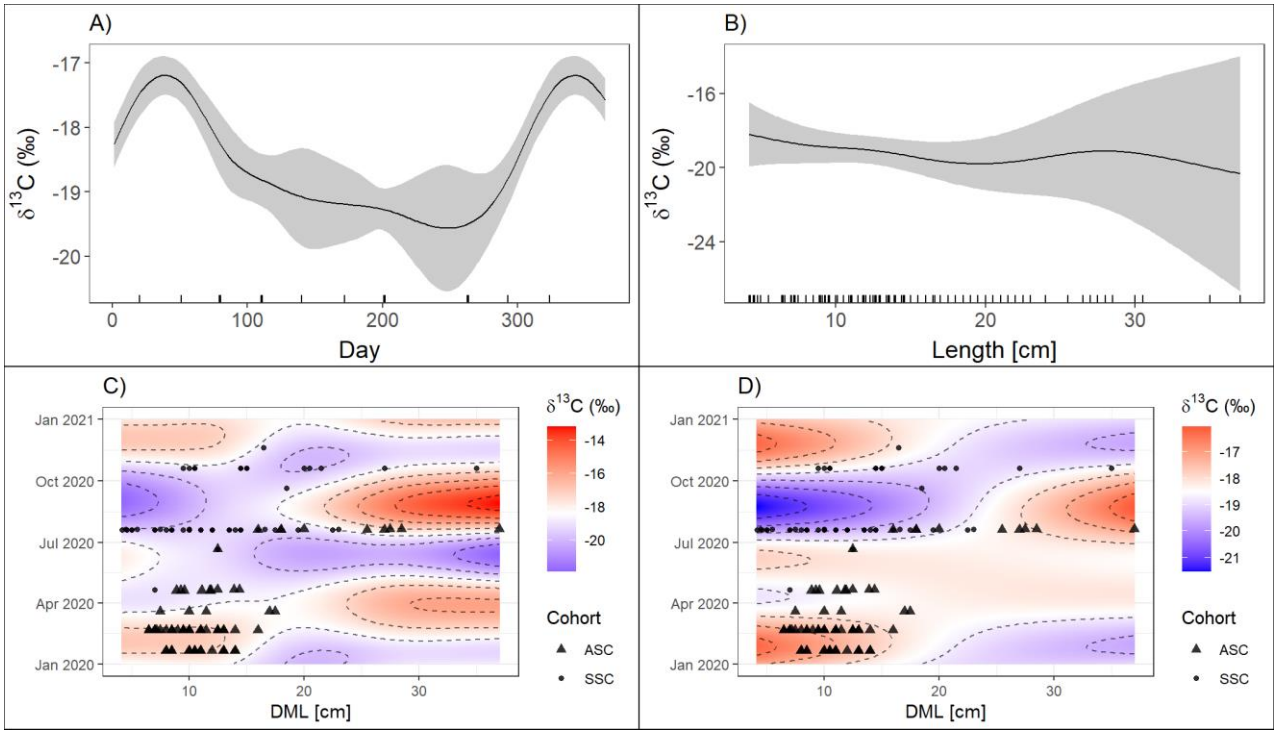

Figure 6. Estimated smoothing curves from the GAMM for $\delta^{13}C$ values of gladius tissue vs. A) DML [cm] and B) day of the year; C): ti-tensor (interaction excluding main effects) of day of the year and DML [cm]; D): te-tensor (interaction including main effects) of day of the year and DML [cm]; triangles = ASC, circles = SSC

Table 3. Mean $\delta^{13}C$ and $\delta^{15}N$ values (‰) with standard deviation and number of samples of Euphausiacea, *Munida gregaria* and salps.

	N	$\delta^{15}N$	$\delta^{13}C$	TL (based on Isoscapes)
Euphausia lucens	3	8.04 ± 1.22	-20.61 ± 0.39	1.81 ± 0.43
Munida gregaria	9	8.80 ± 1.28	-20.24 ± 0.73	2.62 ± 0.61
Salps	1	8.79	-21.88	1.91
Total	13	8.61 ± 1.2	-20.47 ± 0.77	2.38 ± 0.65

The mean $\delta^{15}N$ of the 8 pooled samples of *M. gregaria* was 8.8 ‰. When adding values from Euphausiacea (n=3) and the value from the pooled salp individuals (n=1), the average $\delta^{15}N$ was 8.61. This value as the first method was used as the N baseline value to calculate the trophic

level of *D. gahi* using eq. 2a. However, the trophic level of zooplankton based on isoscapes suggested, that the *M. gregaria* was above trophic level 2 and the average zooplankton baseline slightly above 2. Therefore, we continued our analysis with trophic levels calculated from the isoscape model, which was based on particulate organic matter.

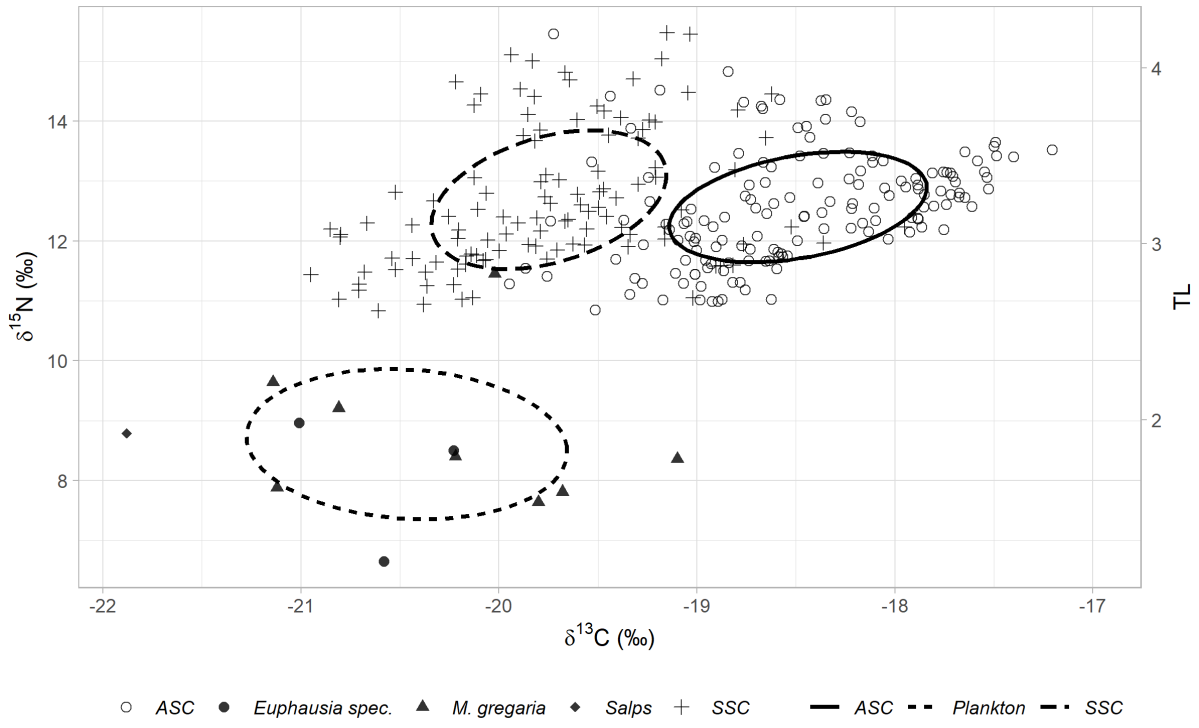

Figure 7. Stable isotope niche of *D. gahi's* spawning cohorts (muscle tissue) with zooplanktonic baseline (Euphausiacea, *M. gregaria* and salps).

3.4. Trophic level based on isoscapes

The linear equation (R^2 = 0.458) for the relationship between $\delta^{15}N$ muscle tissue and $\delta^{15}N$ gladius tissue was found to be:

$$N_{muscle} = 9.70 + 0.363 * \delta^{15}N_{gladius} \; (eq.\ 6)$$

with eq. 6 corrected $\delta^{15}N$ values were calculated for gladius tissue.

Using the $\delta^{15}N$ baseline values from zooplankton (Figure S1 supplementary material) and isoscapes, trophic level for each *D. gahi* individual, each cohort and each size class were calculated. The mean $\delta^{15}N$ for muscle tissue of adult (mature) *D. gahi* individuals was 12.74 (±1.09) ‰, for ASC 12.83 (±1.03) ‰ and for SSC 12.68 (±1.14) ‰. The mean trophic level of adult squid based on zooplankton and muscle tissue was 3.23 (±0.34), for ASC 3.26 (±0.32) and for SSC 3.21 (±0.36), whereas based on isoscapes it was 3.47 (±0.46) overall, for the ASC 3.52 (±0.51) and 3.44 (±0.42) for the SSC. Trophic level increased with size but was similar between cohorts for each size class. Detailed information about $\delta^{15}N$ and trophic level for each cohort and size class per tissue type can be found in Table 4.

Table 4. Mean $\delta^{13}C$ and $\delta^{15}N$ values (‰) and trophic level based on a) zooplankton and b) isoscapes per cohort, tissue (for gladius based on the enrichment factor E) and size-class of *D. gahi* with standard deviation (SD). N = number of individuals

Cohort	Type	Size-class	Mean $\delta^{15}N$ ± SD	Mean $\delta^{13}C$ ± SD	Mean TL (Zooplankton) ± SD	Mean TL (Isoscapes) ± SD	Mean DML ± SD	n
ASC	Muscle	small	12.61 ± 1.03	-18.66 ± 0.4	3.12 ± 0.3	3.43 ± 0.27	6.95 ± 0.75	12
		medium	12.46 ± 0.86	-18.51 ± 0.6	3.08 ± 0.25	3.44 ± 0.50	11.49 ± 2.35	133
		large	13.92 ± 0.43	-18.07 ± 1.21	3.51 ± 0.13	3.77 ± 0.43	26.6 ± 5.10	10
	Gladius	small	8.47 ± 0.89	-17.60 ± 0.64	3.17 ± 0.1	3.41 ± 0.36	7.03 ± 0.42	7
		medium	8.86 ± 1.23	-17.69 ± 1.00	3.21 ± 0.13	3.26 ± 0.55	11.57 ± 2.55	58
		large	10.09 ± 0.61	-17.87 ± 0.36	3.34 ± 0.06	3.27 ± 0.06	27.58 ± 5.51	6
SSC	Muscle	small	12.4 ± 1.13	-19.6 ± 0.82	3.06 ± 0.33	3.51 ± 0.27	5.67 ± 1.13	22
		medium	12.69 ± 1.09	-19.81 ± 0.51	3.14 ± 0.32	3.48 ± 0.41	13.25 ± 3.18	81
		large	13.25 ± 1.51	-19.61 ± 0.63	3.31 ± 0.45	3.40 ± 0.33	24.77 ± 4.77	11
	Gladius	small	7.29 ± 0.86	-19.37 ± 0.85	3.04 ± 0.09	3.44 ± 0.39	5.85 ± 1.26	11
		medium	7.64 ± 1.45	-19.29 ± 0.65	3.08 ± 0.15	3.33 ± 0.42	12.46 ± 3.14	35
		large	8.37 ± 2.18	-19.12 ± 1.27	3.15 ± 0.23	3.36 ± 0.38	24.21 ± 5.28	7

The trophic levels of gladius tissue based on corrected $\delta^{15}N$ values and based on muscle tissue $\delta^{15}N$ values were calculated from the isoscape baselines (with eq. 2b) and analysed (GAM eq. 4, Fig. 8). A clear trend could be seen in both tissues with trophic levels higher in austral winter months (Apr-Oct), although the trend was clearer to observe in muscle tissue.

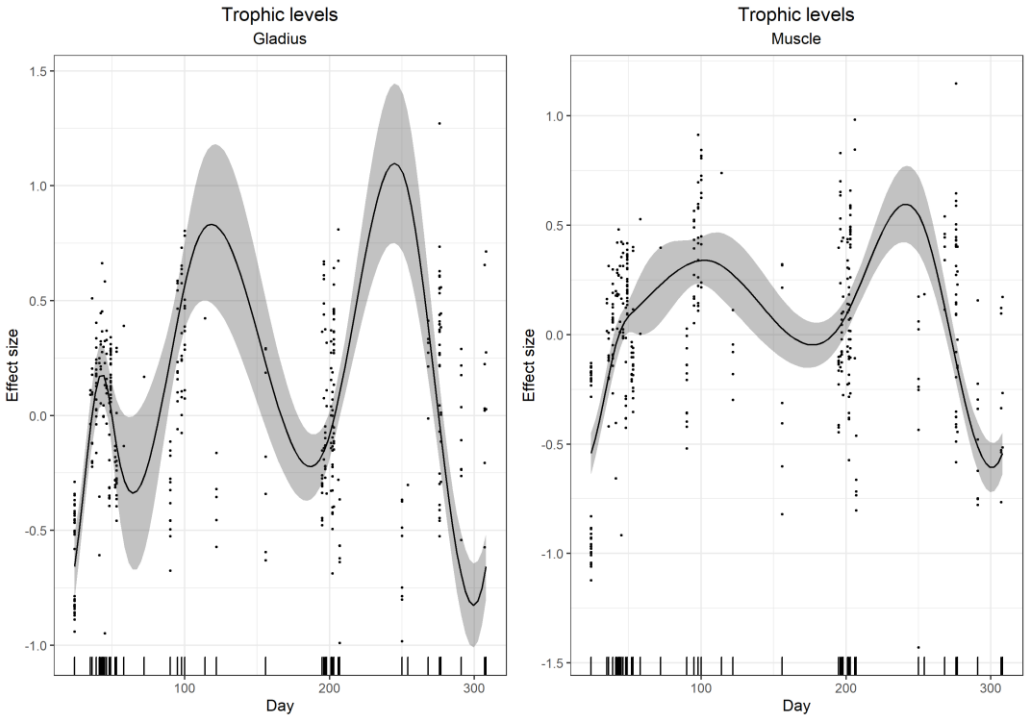

Figure 8. Effect size of trophic levels of *D. gahi* over the year 2020 separate for gladius and muscle tissue. Smoothers for both tissue types were significant ($p<0.001$, edf = 4.96 and edf = 4.87 resp.), as was the intercept (estimate = 3.43, $p<0.001$) and 40.4% of the overall deviance was explained by the model.

3.5. Trophic niche based on SIA

Differences in stable isotope values between muscle and gladius tissue were observed. Gladius $\delta^{15}N$ values were on average 34.1% lower (8.43 ± 1.72 ‰) than muscle tissue (12.8 ± 0.88 ‰)

and $\delta^{13}C$ values were 2.6% higher in the gladius (-18.60 ± 1.20 ‰) compared to muscle tissue (-19.1 ± 0.90 ‰; Fig. 8).

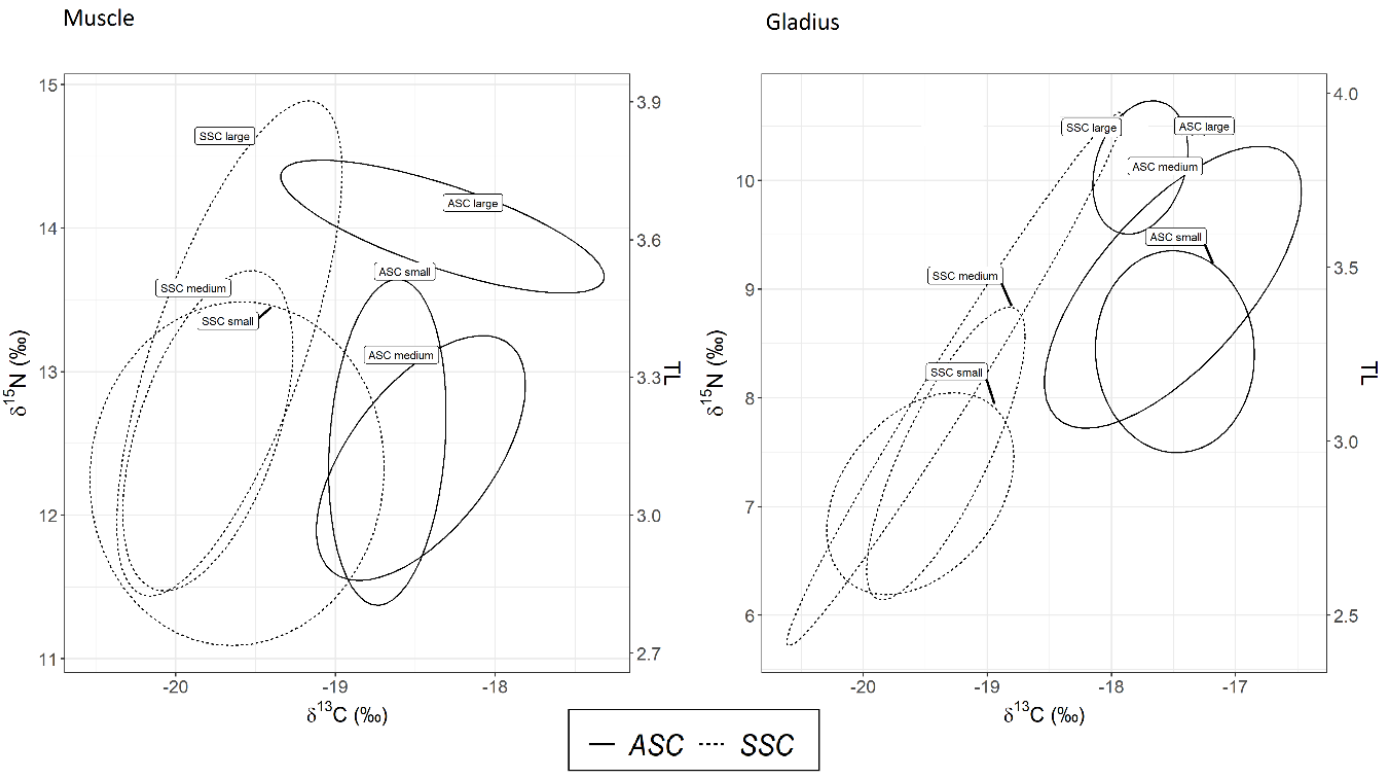

Figure 9. Mean stable isotope signatures $\delta^{13}C$ and $\delta^{15}N$ (‰) and standard ellipse size classes of autumn spawning cohort (ASC, solid line) and spring spawning cohort (SSC, dashed line); left: muscle tissue, right: gladius tissue

Muscle tissue values of $\delta^{13}C$ and $\delta^{15}N$ for each size-class and cohort clustered separately, mainly due to their different $\delta^{13}C$ values (Standard Ellipse Area, Fig. 9). $\delta^{13}C$ values clearly separated both cohorts, where the ASC had values above -19 ‰, whereas the SSC individuals mostly had values below -19 ‰. Both cohorts ranged between 11 and 14 ‰ for $\delta^{15}N$. ASC values clustered around -17.5 and -19.5 ‰ for $\delta^{13}C$ but SSC values clustered around -19.5 and -20.5 ‰ for $\delta^{13}C$ and therefore had a slightly narrower range than the ASC.

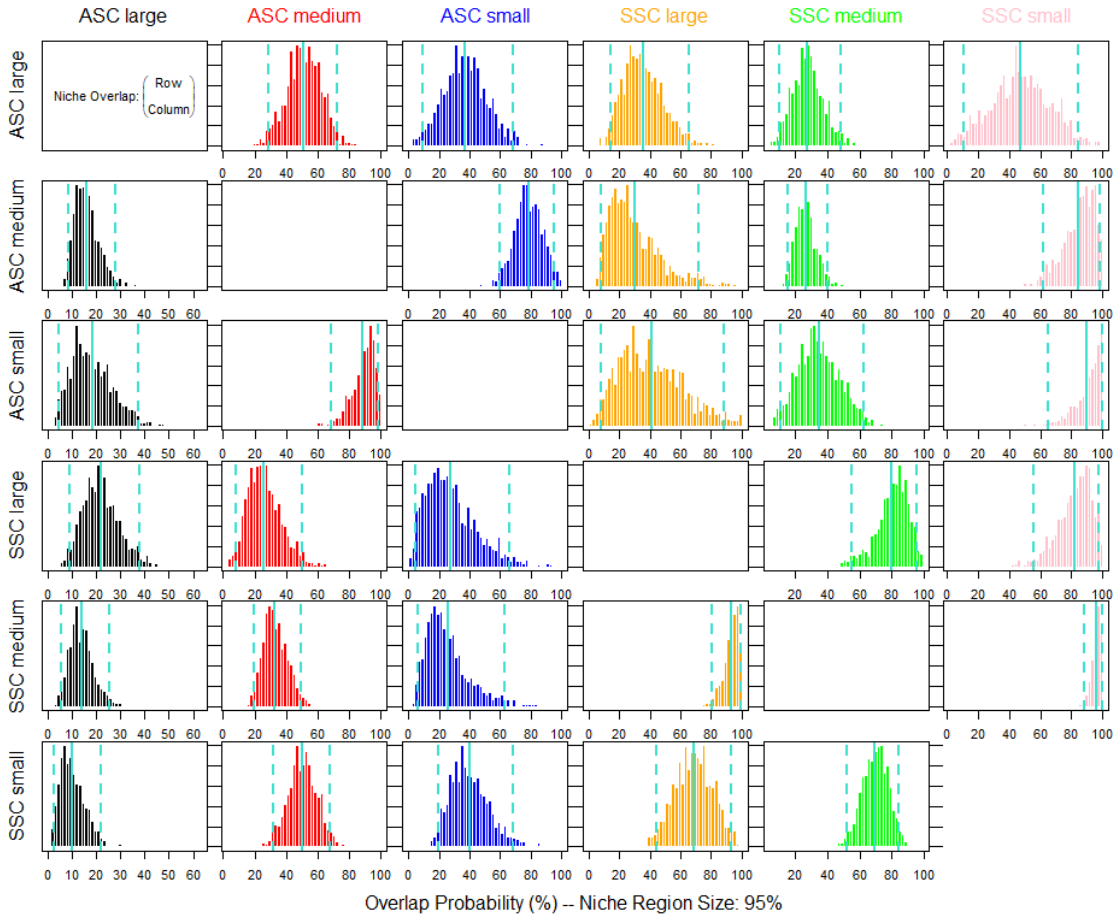

Figure 10: Niche Overlap Probability for each cohort and size class at a 95% alpha level for muscle tissue

Trophic niche of small and medium-sized squid based on muscle tissue overlapped for each spawning cohort (Fig. 9). Highest mean niche overlap in muscle tissue (Fig. 10, Table S2 supplementary material) had the group SSC medium with SSC small (95.77%) and with SSC large (92.58%). ASC small had a high overlap with SSC small (90.5%) and with ASC medium (88.52%). Least overlap had ASC large with SSC small (10.29%) and with SSC medium (14.21%), followed by ASC medium (16.32%) and ASC small (18.46%).

Like muscle tissue, the main difference in gladius tissue between cohorts was seen in the $\delta^{13}C$ values, whereas $\delta^{15}N$ values were similar in both cohorts. Gladius SSC values clustered between -20 and -18.5 ‰ for $\delta^{13}C$ and between 6 and 11 ‰ for $\delta^{15}N$. ASC gladius values clustered between -18.5 and ~-16.3 ‰ for $\delta^{13}C$. The $\delta^{15}N$ cluster of the ASC gladius values

were narrower compared to the SSC with values between 8 and 11 ‰. Trophic niche as assessed by gladius tissue looked very similar to that based on muscle tissue, but with large SSC individuals having a wider niche in $\delta^{13}C$ and large ASC individuals having a narrower $\delta^{13}C$ niche (Fig. 9). Large SSC individuals had a large spread in $\delta^{15}N$ in both muscle and gladius tissues, from about 6 to 11 ‰.

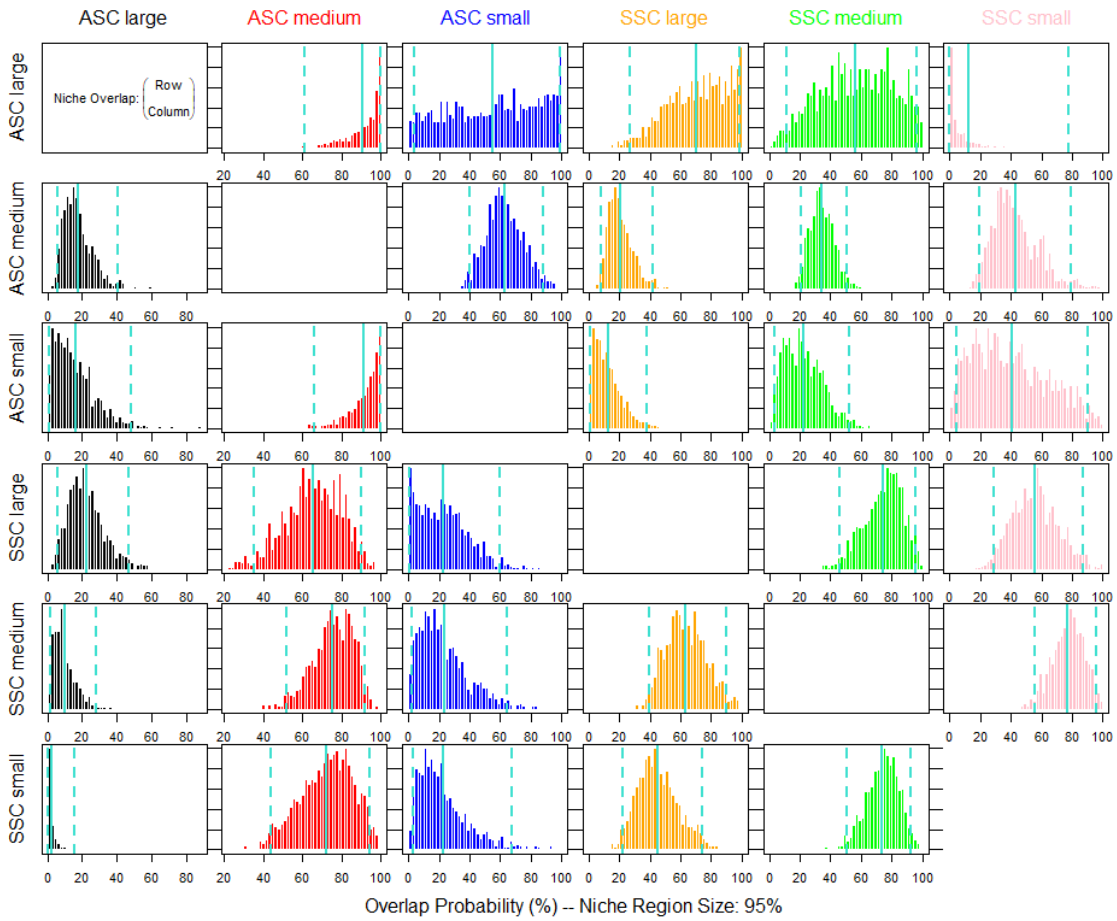

Figure 11. Niche Overlap Probability for each cohort and size class at a 95% alpha level for gladius tissue.

Regarding the niche overlap in gladius tissue (Fig. 11, Table S2), the group ASC medium had the highest overlaps with ASC large (90.61%) and with ASC small (90.33%), followed by SSC medium overlapping with SSC small (77.61%) and ASC medium (75.03%). Least mean niche overlap was found again in ASC large with SSC mall (2.73%) and SSC medium (9.94%),

followed by SSC small overlapping with ASC large (12.35%) and ASC small overlapping with SSC large (13.25%).

The standard ellipse areas (representing the isotopic niche) and the niche overlap estimated with Bayesian procedures clearly differed for squids of different size groups, with the group ASC large having least niche overlap with other groups in muscle and gladius tissue. Group SSC small had the largest niche overlaps in muscle tissue, whereas group ASC medium showed the largest niche overlaps in gladius tissue (Figs. 9 to 11).

4. Discussion

This study represents the first attempt to investigate the trophic niches of two seasonal cohorts of *Doryteuthis gahi* using stable isotope analysis, with samples of muscle to indicate recent diet (weeks) and samples of gladius to represent diet over a longer time-scale (months). Inclusion of the Area as a mixed effect factor improved the models, however we did not investigate further the spatial differences in this study and left them for further studies.

As expected, $\delta^{15}N$ and the related trophic level increased with increasing body size. This was shown in many other squid species such as the ommastrephid squid *Dosidicus gigas* (Ruiz-Cooley et al., 2006), the gonatid squid *Gonatus fabricii* (Golikov et al., 2018), and in *D. gahi* (Rosas-Luis et al., 2017). Büring et al. (2022) found a size-dependent diet change in *D. gahi*. Small individuals of *D. gahi* fed on Euphausiacea, whereas larger individuals were found to prey upon fish such as Myctophidae or on small squid, including cannibalism (Büring et al., 2022; Rosas-Luis et al., 2014). These variations in diet reflect the development of morphological features related to feeding, e.g. growth of arms and tentacles, or the beak (Boucher-Rodoni et al., 1987). Larger sized individuals are feeding on larger prey, which itself

occupies higher trophic levels (Boucher-Rodoni et al., 1987). Larger individuals were sampled in the ASC (+ 2 cm larger on average), which could be one factor explaining the very distinct niche of large ASC individuals. The model fit was lowest for muscle tissue $\delta^{15}N$ values explained by DML of squid.

In a prior analysis on aged *D. gahi* individuals, based on statolith growth increment counts averaged from the last 20 years, it was found that for squid measuring 10 cm DML, the last fifth part of the gladius represented approximately the last 41 days (±3 days) of squid life, in 20 cm DML squid ~the last 51 days (±4 days) and in 30 cm DML squid ~the last 53 days (±8 days) (Falkland Islands Government - unpublished data). Therefore, the gladius tissue of the ASC might have preserved the summer peak in $\delta^{15}N$, whereas the ASC muscle tissue reflects lower autumn $\delta^{15}N$ values and their feeding at the lower trophic levels. In the SSC, these contrasting effects of feeding on higher trophic level prey (Amphipods, Chaetognaths, fish and squid) on the one hand but experiencing a lower $\delta^{15}N$ baseline in winter months and in greater water depths on the other hand, might have balanced each other out. The results were similar in $\delta^{15}N$ muscle values of the SSC compared to the ASC but the SSC was lacking the $\delta^{15}N$ summer peak evident in the gladius tissue of the ASC, which might be therefore lower compared to the ASC. Results of trophic levels based on the isoscape baseline (Figure 8) confirmed higher trophic levels in winter months despite lower $\delta^{15}N$ values and are in agreement with findings of the diet study by Büring et al. (2022).

Highly productive areas such as the Patagonian Shelf seem to cause an increased uptake of nitrates by phytoplankton, resulting in high $\delta^{15}N$ isoscapes. St John Glew et al. (2021) modelled nitrogen isoscapes of the Southern Ocean and found $\delta^{15}N$ to be dependent on the distance to the coast and water depth. The authors isoscape models predicted higher $\delta^{15}N$ values during the summer months (Nov-Dec) compared to the winter months (May-Oct) for the Southern Ocean and around continental shelves of the South Atlantic. Considering the results of the diet

study from Büring et al., (2022), the SSC were expected to have higher $\delta^{15}N$ values (for both muscle and gladius tissue) due to a diet consisting of species of higher trophic level (Chaetognatha, Amphipoda, fish). This was not reflected in this study. Instead, the ASC was found to have similar muscle tissue values, higher gladius $\delta^{15}N$ values and occupied a higher trophic level when compared to the SSC. Therefore, not only must the diet composition of each cohort be considered but also the overall trophic baseline each cohort experiences throughout its development.

The most pronounced difference in stable isotope values between the two spawning cohorts of *D. gahi* was $\delta^{13}C$. Carbon stable isotope values are based on primary producers, altering very little within the food chain (Cherel and Hobson, 2007; DeNiro and Epstein, 1978; Tieszen et al., 1983) and are influenced by environmental factors such as temperature, light intensity and currents (France, 1995). As our models accounted for potential spatial variability, the differences in $\delta^{13}C$ values found between the two seasonal spawning cohorts of *D. gahi* were most likely to reflect seasonal differences in $\delta^{13}C$ values of primary producers of the Patagonian Shelf ecosystem. The ASC feed during the austral summer and therefore in warmer and shallower shelf waters compared to the SSC, which have their feeding period during the austral winter and occur at deeper depths (Arkhipkin et al., 2013, 2004). This might explain the lower $\delta^{13}C$ values in muscle and gladius tissues of the SSC, as deeper offshore waters are normally more depleted in $\delta^{13}C$ than more productive coastal waters (Miller et al., 2008). Furthermore, Quillfeldt et al. (2015) found seasonal variability in $\delta^{13}C$ and $\delta^{15}N$ around the Falkland Islands, with higher $\delta^{13}C$ values in summer than in spring, supporting the findings of this study.

Muscle and gladius tissues had distinct stable isotope values. It is known that cephalopod muscle tissue is normally low in lipids but is rich in proteins (Clarke et al., 1994). Apart from proteins, cephalopod hard structures such as beaks or gladius are mainly composed of chitin, which is a polymer of N-acetyl-b-D-glucosamine (Arkhipkin et al., 2012; Merzendorfer and

Zimoch, 2003). Chitin and purified D-glucosamine of arthropod exoskeletons were found to have lower $\delta^{15}N$ ratios compared to muscle tissue; however, similar to muscle tissue, $\delta^{15}N$ ratios of gladius tissue increased with increasing trophic level (Schimmelmann and DeNiro, 1986). $\delta^{13}C$ values vary little between tissue types (Cherel and Hobson, 2005; Schimmelmann and DeNiro, 1986), due to the different composition of amino acids in hard structures (lacking protein) and muscle tissue (pure protein in the case of cephalopods; (Cherel et al., 2019, 2009). *Loligo* sp. were found to have chitin to protein ratios of about 1:2 to 1:1.5 in the gladius (Hunt and Nixon, 1981), which we can assume is similar to our study species *D. gahi*. Cherel and Hobson (2005) found higher $\delta^{15}N$ values in muscle tissue compared to $\delta^{15}N$ depleted beaks, due to different metabolic pathways for protein and chitin. In this study, gladius tissue was less enriched in ^{15}N and ^{13}C than muscle tissue, but both showed similar trends in seasonality and for $\delta^{15}N$ also in size.

To estimate the trophic level of two cohorts in three different size groups, the trophic baseline of the Patagonian shelf ecosystem was calculated based on $\delta^{15}N$ values of primary consumers of phytoplankton and on modelled isoscapes by St John Glew et al. (2021). In this study Euphausiacea, larval and juvenile plankton stages of the lobster krill *M. gregaria* and salps were sampled during the same year, even though not all seasons and areas could be sampled evenly. The use of salps to determine the trophic baseline is contested (Stowasser et al., 2012) as they consume flagellates and cyanobacteria (i.e. *Prochlorococcus*) (Sutherland et al., 2010; von Harbou et al., 2011), which are isotopically depleted compared to large phytoplankton (Del Giorgio and France, 1996; Fawcett et al., 2010; Fry and Wainright, 1991). Selective feeding on flagellates and cyanobacteria could lead to lower isotopic signatures of salps compared to those found for particulate organic matter. Zooplankton species follow a strong seasonal pattern, with highest abundances in spring and summer (Sabatini and Colombo, 2001). This study has the constraints of not covering SI values of zooplankton throughout the whole year

of 2020 to access seasonality of primary consumers. Values obtained from autumn and spring were averaged that prevented to describe seasonality.

The trophic level of a species may alter over time or be different in different ecosystems, but rather than using only $\delta^{15}N$ values, the trophic level enables us to compare species and studies in a more standardized way (Navarro et al., 2013). On the one hand, using Euphausiacea and Munida specimens sampled within the same year and area as the target species (*D. gahi*) to calculate trophic level seemed very important. But on the other hand, the use of isoscapes, specific for each location and moment of time seemed more reliable due to relative scarcity of our zooplankton samples. According to the isoscapes calculated by St John Glew et al. (2021), euphausiids and salps had a trophic level of about 2, whereas *M. gregaria* planktonic juveniles had slightly higher levels.

Highest niche overlaps based on muscle tissue isotopes were revealed for the SSC cohort, especially the small individuals with medium and large ones, as well as with ASC small and medium individuals. As the SSC has a shortened egg development time and faster growth rate due to warm temperatures in austral summer months, they can be found in the same water column at the same time (Arkhipkin et al., 2004), hence sharing the same ecotrophic niche. On the other hand, large ASC individuals can be found late in austral winter months (May-July), being the only group in Falkland Island waters with little sharing of their trophic niche with other groups, due to the specific environmental conditions this group is exposed to. Apart from their sampling size, this would be another factor, explaining the unique econiche of this group.

Classical stomach content analysis may be biased due to factors e.g. rejecting hard parts such as bones, otoliths and beaks, overestimating the importance of soft-tissue items such as crustaceans (Boyle and Rodhouse, 2005; Buckland et al., 2017). Nevertheless, stomach content analysis has advantages when it comes to the identification of prey species compared to SIA,

as the latter can only predict possible prey species and are highly dependent on good SI mixing models including all possible prey items (Bearhop et al., 2004; Hyslop, 1980; Jackson et al., 2011; Montecinos et al., 2016). A combination of both methods might achieve the best results when determining the ecology and trophic position of a species (Martínez-Baena et al., 2016; Rosas-Luis et al., 2016). This study with the SIA approach supports the findings of Büring et al., (2022). The spawning cohorts of *D. gahi* might have distinct trophic niches due to the different environmental factors such as depth and temperature regimes (e.g. carbon baselines) the cohorts experience during their lifetime (Arkhipkin et al., 2004).

This study made a further contribution towards understanding the ecology of the two spawning cohorts of *D. gahi*. The knowledge of the ecotrophic niches and trophic levels of two seasonal spawning cohorts of a squid species can provide important information for ecosystem-based management. It will help to better understand the role of *D. gahi* in the ecosystem and its relationships with other species and to predict the impacts of changes in the environment on *D. gahi* and the ecosystem as a whole. Furthermore, it will help developing effective management strategies to conserve *D. gahi* and maintain the ecological balance of the ecosystem.

Acknowledgements. We would like to thank the scientific fisheries observers of the Falkland Islands Fisheries Department for collecting samples. We would like to thank the South Atlantic Environmental Research Institute (SAERI) for supporting this work with the sampling of zooplankton species. The University of Vigo is to thank for supporting this PhD project. The authors are grateful to Gaël Guillou and Gauthier Poiriez from the platform «Analyses Isotopiques» of LIENSs for their help with stable isotope analyses. The Institut Universitaire de France is to acknowledged for its support to Paco Bustamante as a Senior Member.

Financial support

The Beauchene Ltd Fishing Company is to thank for part-sponsored this study along with the Falkland Island Fisheries Department. The Director of the Fisheries Department, Dr Andrea Clausen is to thank for supporting this research. The CPER (Contrat de Projet Etat-Région) and the FEDER (Fonds Européen de Développement Régional) are acknowledged for funding the IR-MS of LIENSs laboratory.

References

Acha, E.M., Mianzan, H.W., Guerrero, R.A., Favero, M., Bava, J., 2004. Marine fronts at the continental shelves of austral South America. Journal of Marine Systems 44, 83–105. https://doi.org/10.1016/j.jmarsys.2003.09.005

Arkhipkin, A.I., Bizikov, V.A., Fuchs, D., 2012. Vestigial phragmocone in the gladius points to a deepwater origin of squid (Mollusca: Cephalopoda). Deep-Sea Research Part I 61, 109–122. https://doi.org/10.1016/j.dsr.2011.11.010

Arkhipkin, A.I., Grzebielec, R., Sirota, A.M., Remeslo, A. V., Polishchuk, I.A., Middleton, D.A.J., 2004. The influence of seasonal environmental changes on ontogenetic migrations of the squid *Loligo gahi* on the Falkland shelf. Fisheries Oceanography 13, 1–9. https://doi.org/10.1046/j.1365-2419.2003.00269.x

Arkhipkin, A.I., Hatfield, E.M.C., Rodhouse, P.G.K., 2013. *Doryteuthis gahi*, Patagonian Long-Finned Squid, in: Rosa, R., O'Dor, R., Pierce, G. (Eds.), Advances in Squid Biology, Ecology and Fisheries. Part 1. Nova Science Publisher, Inc., pp. 123–157.

Bearhop, S., Adams, C.E., Waldron, S., Fuller, R.A., Macleod, H., 2004. Determining trophic niche width: a novel approach using stable isotope analysis. Journal of Animal Ecology 73, 1007–1012.

Boltovskoy, D., 1999. South Atlantic Zooplanton , Volume 2. Backhuys Publisher.

Boucher-Rodoni, R., Boucaud-Camou, E., Mangold, K., 1987. Feeding and digestion, in: Boyle, P.R. (Ed.), In Boyle PR (Ed) Cephalopod Life Cycles. Comparative Reviews Vol. 2. London, Orlando, Academic Press, pp. 85–108.

Boyle, P., Rodhouse, P.G.K., 2005. Ecology and Fisheries. Blackwell Science, Oxford, UK.

Brickle, P., Olson, P.D., Littlewood, D.T.J., Bishop, A., Arkhipkin, A.I., 2002. Parasites of *Loligo gahi* from waters off the Falkland Islands , with a phylogenetically based identification of their cestode larvae. Canadian Journal of Zoology 79, 2289–2296. https://doi.org/10.1139/cjz-79-12-2289

Buckland, A., Baker, R., Loneragan, N., Sheaves, M., 2017. Standardising fish stomach content analysis: The importance of prey condition. Fisheries Research 196, 126–140. https://doi.org/10.1016/j.fishres.2017.08.003

Büring, T., Schroeder, P., Jones, J.B., Pierce, G.J., Rocha, F., Arkhipkin, A.I., 2022. Size-related, seasonal and interdecadal changes in the diet of the Patagonian longfin squid *Doryteuthis gahi* in the Southwestern Atlantic. Journal of the Marine Biological Association of the United Kingdom 1–18. https://doi.org/10.1017/S0025315422000194

Cabana, G., Rasmussen, J.B., 1996. Comparison of aquatic food chains using nitrogen isotopes. Proceedings of the National Academy of Sciences of the United States of America 93, 10844–10847.

Castro, L.R., González, H.E., Garcés-Vargas, J., Barrientos, P., 2021. Separate Feeding Between the Pelagic Stage of the Squat Lobster *Munida gregaria* and the Larger Sized Zooplankton Crustacean Groups in the Beagle Channel as Revealed by Stable Isotopes. Frontiers in Marine Science 8. https://doi.org/10.3389/fmars.2021.635190

Cherel, Y., Bustamante, P., Richard, P., 2019. Amino acid δ13C and δ15N from sclerotized beaks: a new tool to investigate the foraging ecology of cephalopods , including giant and colossal squids. Marine Ecology Progress Series 624, 89–102. https://doi.org/10.3354/meps13002

Cherel, Y., Ducatez, S., Fontaine, C., Richard, P., Guinet, C., 2008. Stable isotopes reveal the trophic position and mesopelagic fish diet of female southern elephant seals breeding on the Kerguelen Islands. Marine Ecology Progress Series 370, 239–247. https://doi.org/10.3354/meps07673

Cherel, Y., Fontaine, C., Jackson, G.D., Jackson, C.H., Richard, P., 2009. Tissue, ontogenic and sex-related differences in δ13C and δ15N values of the oceanic squid Todarodes filippovae (Cephalopoda: Ommastrephidae). Marine Biology 156, 699–708. https://doi.org/10.1007/s00227-008-1121-x

Cherel, Y., Hobson, K.A., 2007. Geographical variation in carbon stable isotope signatures of marine predators: a tool to investigate their foraging areas in the Southern Ocean. Marine Ecology Progress Series 329, 281–287.

Cherel, Y., Hobson, K.A., 2005. Stable isotopes, beaks and predators: a new tool to study the trophic ecology of cephalopods, including giant and colossal squids. Proceedings of the Royal Society B: Biological Sciences 272, 1601–1607. https://doi.org/10.1098/rspb.2005.3115

Clarke, A., Rodhouse, P.G., Gore, D.J., 1994. Biochemical composition in relation to the energetics of growth and sexual maturation in the ommastrephid squid *Illex argentinus*. Philosophical Transactions of the Royal Society B: Biological Sciences 344, 201–212. https://doi.org/10.1098/rstb.1994.0061

Coll, M., Navarro, J., Olson, R.J., Christensen, V., 2013. Assessing the trophic position and ecological role of squids in marine ecosystems by means of food-web models. Deep-Sea Research Part II: Topical Studies in Oceanography 95, 21–36. https://doi.org/10.1016/j.dsr2.2012.08.020

Del Giorgio, P.A., France, R.L., 1996. Ecosystem-specific patterns in the relationship between zooplankton and POM or microplankton δ13C. Limnology and Oceanography 41, 359–365. https://doi.org/10.4319/lo.1996.41.2.0359

DeNiro, M.J., Epstein, S., 1978. Influence of diet on the distribution of carbon isotopes in animals. Geochimica et Cosmochimica Acta 42, 495–506. https://doi.org/10.1016/0016-7037(78)90199-0

Fawcett, S.E., Lomas, M.W., Ward, B.B., Casey, J.R., Sigman, D.M., 2010. Eukaryotes dominate new production in the Sargasso Sea. Geochimica et Cosmochimica Acta 1405, 96822–96822.

France, R.L., 1995. Carbon-13 enrichment in benthic compared to planktonic algae: foodweb implications. Marine Ecology Progress Series 124, 307–312.

Fry, B., 2006. Stable isotope ecology, 521st ed. Springer, New York.

Fry, B., Wainright, S.C., 1991. Diatom sources of 13C-rich carbon in marine food webs. Marine Ecology Progress Series 76, 149–157. https://doi.org/10.3354/meps076149

Gasalla, M.A., Rodrigues, A.R., Postuma, F.A., 2010. The trophic role of the squid Loligo plei as a keystone species in the South Brazil Bight ecosystem. ICES Journal of Marine Science 67, 1413–1424. https://doi.org/10.1093/icesjms/fsq106

Gibbons, M.J., Barange, M., Pillar, S.C., 1991. Vertical migration and feeding of *Euphausia lucens* (Euphausiacea) in the Southern Benguela. Journal of Plankton Research 13, 473–486.

Golikov, A. V., Ceia, F.R., Sabirov, R.M., Zaripova, Z.I., Blicher, M.E., Zakharov, D. V., Xavier, J.C., 2018. Ontogenetic changes in stable isotope (δ13C and δ15N) values in squid *Gonatus fabricii (Cephalopoda)* reveal its important ecological role in the Arctic. Marine Ecology Progress Series 606, 65–78. https://doi.org/10.3354/meps12767

Grisley, M.S., Boyle, P.R., 1988. Recognition of food in *Octopus* digestive tract. Journal of Experimental Marine Biology and Ecology 118, 7–32. https://doi.org/10.1016/0022-0981(88)90119-0

Grisley, M.S., Boyle, P.R., 1985. A new application of serological techniques to gut content analysis. Journal of Experimental Biology and Ecology 90, 1–9. https://doi.org/doi.org/10.1016/0022-0981(85)90070-X

Guerra, A., Castro, B.G., Nixon, M., 1991. Preliminary study on the feeding by *Loligo gahi* (Cephalopoda: Loliginidae). Bulletin of Marine Science 49, 309–311.

Guerreiro, M., Phillips, R.A., Cherel, Y., Ceia, F.R., Alvito, P., Rosa, R., Xavier, J.C., 2015. Habitat and trophic ecology of Southern Ocean cephalopods from stable isotope analyses. Marine Ecology Progress Series 530, 119–134. https://doi.org/10.3354/meps11266

Hastie, T., Tibshirani, R., 1986. Generalized Additive Models. Statistical Science 1, 297–318.

Hunt, S., Nixon, M., 1981. A comparative study of protein composition in the chitin-protein complexes of the beak, pen, sucker disc, radula and oesophageal cuticle of cephalopods. Comparative Biochemistry and Physiology 68, 535–546. https://doi.org/10.1016/0305-0491(81)90071-7

Hyslop, E.J., 1980. Stomach contents analysis-a review of methods and their application. Journal of Fish Biology 17, 411–429.

Jackson, A.L., Inger, R., Parnell, A.C., Bearhop, S., 2011. Comparing isotopic niche widths among and within communities: SIBER - Stable Isotope Bayesian Ellipses in R. Journal of Animal Ecology 80, 595–602. https://doi.org/10.1111/j.1365-2656.2011.01806.x

Jaeger, A., Lecomte, V.J., Weimerskirch, H., Richard, P., Cherel, Y., 2010. Seabird satellite tracking validates the use of latitudinal isoscapes to depict Seabird satellite tracki ng validates the use of latitudinal isoscapes to depict predators ' foraging areas in the Southern Ocean. Rapid Communications in Mass Spectrometry 24, 3456–3460. https://doi.org/10.1002/rcm.4792

Jereb, P., Roper, C.F.E. (Eds.), 2010. Cephalopods of the world: an annotated and illustrated catalogue of cephalopod species known to date, FAO species catalogue for fishery purposes. Food and Agriculture Organization of the United Nations, Rome.

Jones, J.B., Arkhipkin, A.I., Marriott, A.L., Pierce, G.J., 2018. Using statolith elemental signatures to confirm ontogenetic migrations of the squid *Doryteuthis gahi* around the Falkland Islands (Southwest Atlantic). Chemical Geology 481, 85–94. https://doi.org/10.1016/j.chemgeo.2018.01.034

Lipinski, M.R., 1979. Universal maturity scale for the commercially important squid (Cephalopoda: Teuthoidea). The results of maturity classifications of the *Illex illecebrosus* (LeSueur, 1821) populations for the years 1973–1977. International Commission for the Northwest Atlantic Fisheries (ICNAF) Research Documents 79, 40.

Lysy, M., Stasko, A.D., Swanson, H.K., 2021. Overlap Metrics for Multidimensional Ecological Niches. R package.

Markaida, U., Sosa-Nishizaki, O., 2003. Food and feeding habits of jumbo squid *Dosidicus gigas* (Cephalopoda: Ommastrephidae) from the Gulf of California, Mexico. Journal of the Marine Biological Association of the United Kingdom 83, 507–522. https://doi.org/10.1017/S0025315403007434h

Martínez-Baena, F., Navarro, J., Albo-Puigserver, M., Palomera, I., Rosas-Luis, R., 2016. Feeding habits of the short-finned squid *Illex coindetii* in the western Mediterranean Sea using combined stomach content and isotopic analysis. Journal of the Marine Biological Association of the United Kingdom 96, 1235–1242. https://doi.org/10.1017/S0025315415001940

McCutchan, J.H., Lewis, W.M., Kendall, C., McGrath, C.C., 2003. Variation In Trophic Shift for Stable Isotope Ratios of Carbon, Nitrogen, and Sulfur. Oikos 102, 378–390. https://doi.org/10.1034/j.1600-0706.2003.12098.x

Merzendorfer, H., Zimoch, L., 2003. Chitin metabolism in insects: Structure, function and regulation of chitin synthases and chitinases. Journal of Experimental Biology 206, 4393–4412. https://doi.org/10.1242/jeb.00709

Miller, T.W., Brodeur, R.D., Rau, G.H., 2008. Carbon stable isotopes reveal relative contribution of shelf-slope production to the northern California Current pelagic community. Limnology and Oceanography 53, 1493–1503. https://doi.org/10.4319/lo.2008.53.4.1493

Minagawa, M., Wada, E., 1984. Stepwise enrichment of 15N along food chains: Further evidence and the relation between δ15N and animal age. Geochimica et Cosmochimica Acta 48, 1135–1140. https://doi.org/10.1016/0016-7037(84)90204-7

Montecinos, S., Castro, L.R., Neira, S., 2016. Stable isotope (δ13C and δ15N) and trophic position of Patagonian sprat (*Sprattus fuegensis*) from the Northern Chilean Patagonia. Fisheries Research 179, 139–147. https://doi.org/10.1016/j.fishres.2016.02.014

Navarro, J., Coll, M., Somes, C.J., Olson, R.J., 2013. Trophic niche of squids: Insights from isotopic data in marine systems worldwide. Deep-Sea Research Part II: Topical Studies in Oceanography 95, 93–102. https://doi.org/10.1016/j.dsr2.2013.01.031

Perissinotto, R., Pakhomov, E.A., 1998. The trophic role of the tunicate *Salpa thompsoni* in the Antarctic marine ecosystem. Journal of Marine Systems 17, 361–374. https://doi.org/10.1016/S0924-7963(98)00049-9

Phillips, D.L., Inger, R., Bearhop, S., Jackson, A.L., Moore, J.W., Parnell, A.C., Semmens, B.X., Ward, E.J., 2014. Best practices for use of stable isotope mixing models in food-web studies. Can. J. Zool. 92, 823–835. https://doi.org/10.1139/cjz-2014-0127

Pierce, G.J., Boyle, P.R., Hastie, L.C., Santos, M.B., 1994. Diets of squid *Loligo forbesi* and *Loligo vulgaris* in the northeast Atlantik. Fisheries Research 21, 149–163.

Porteiro, F.M., Goncalves, J.M., Cardigos, F., Martins, H.R., 1995. The Azorean squid \textlessi\textgreaterLoligo forbesi\textless/i\textgreater (Cephalopoda: Loliginidae) in captivity: feeding and growth . International Council for the Exploration of the Sea (CM Papers and Reports), 12.

Post, D.M., 2002. Using Stable Isotopes to Estimate Trophic Position: Models , Methods , and Assumptions. Ecology 83, 703–718.

Quillfeldt, P., Ekschmitt, K., Brickle, P., Mcgill, R.A.R., Wolters, V., Dehnhard, N., Masello, J.F., 2015. Variability of higher trophic level stable isotope data in space and time – a case study in a marine ecosystem. Rapid Communications in Mass Spectrometry 29, 667–674. https://doi.org/10.1002/rcm.7145

R Core Team, 2020. R: A language and environment for statistical computing. R Foundation for Statistical.

Rodhouse, P.G., Nigmatullin, Ch.M., 1996. Role as Consumers P. Philosophical Transactions: Biological Sciences 351, 1003–1022.

Rosas-Luis, R., Navarro, J., Martínez-Baena, F., Sánchez, P., 2017. Differences in the trophic niche along the gladius of the squids *Illex argentinus* and *Doryteuthis gahi* based on their isotopic values. Regional Studies in Marine Science 11, 17–22. https://doi.org/10.1016/j.rsma.2017.02.003

Rosas-luis, R., Navarro, J., Sánchez, P., Del Río, J.L., 2016. Assessing the trophic ecology of three sympatric squid in the marine ecosystem off the Patagonian Shelf by combining stomach content and stable isotopic analyses. Marine Biology Research 12, 402–411. https://doi.org/10.1080/17451000.2016.1142094

Rosas-Luis, R., Sánchez, P., Portela, J.M., Del Rio, J.L., 2014. Feeding habits and trophic interactions of *Doryteuthis gahi*, *Illex argentinus* and *Onykia ingens* in the marine ecosystem off the Patagonian Shelf. Fisheries Research 152, 37–44. https://doi.org/10.1016/j.fishres.2013.11.004

Ruiz-Cooley, R., Gendron, D., Aguíñiga, S., Mesnick, S., Carriquiry, J., 2004. Trophic relationships between sperm whales and jumbo squid using stable isotopes of C and N. Mar. Ecol. Prog. Ser. 277, 275–283. https://doi.org/10.3354/meps277275

Ruiz-Cooley, R.I., Gerrodette, T., Chivers, S.J., Danil, K., 2021. Cooperative feeding in common dolphins as suggested by ontogenetic patterns in δ^{15}N bulk and amino acids. J Anim Ecol 90, 1583–1595. https://doi.org/10.1111/1365-2656.13478

Ruiz-Cooley, R.I., Markaida, U., Gendron, D., Aguíñiga, S., 2006. Stable isotopes in jumbo squid (*Dosidicus gigas*) beaks to estimate its trophic position: Comparison between stomach contents and stable isotopes. Journal of the Marine Biological Association of the United Kingdom 86, 437–445. https://doi.org/10.1017/S0025315406013324

Ruiz-Cooley, R.I., Villa, E.C., Gould, W.R., 2010. Ontogenetic variation of δ13C and δ15N recorded in the gladius of the jumbo squid *Dosidicus gigas*: geographic differences. Marine Ecology Progress Series 399, 187–198. https://doi.org/10.3354/meps08383

Sabatini, M.E., Colombo, G.L.Á., 2001. Seasonal pattern of zooplankton biomass in the Argentinian shelf off Southern Patagonia (45 ° -55 ° S)*. Scientia Marina 65, 21–31.

Schimmelmann, A., DeNiro, M.J., 1986. Stable Isotopic Studies on Chitin, Measurements on Chitin/Chitosan Isolates and D-Glucosamine Hydrochloride from Chitin, in: Muzarelli, R., Jeuniaux, C., Gooday, G.W. (Ed.), Chitin in Nature and Technology. Springer, Boston, MA, Boston. https://doi.org/10.1007/978-1-4613-2167-5_43

Somes, C.J., Schmittner, A., Galbraith, E.D., Lehmann, M.F., Altabet, M.A., Montoya, J.P., Letelier, R.M., Mix, A.C., Bourbonnais, A., Eby, M., 2010. Simulating the global distribution of nitrogen isotopes in the ocean. Global Biogeochemical Cycles 24, 1–16. https://doi.org/10.1029/2009GB003767

St John Glew, K., Espinasse, B., Hunt, B.P.V., Pakhomov, E.A., Bury, S.J., Pinkerton, M., Nodder, S.D., Gutiérrez-Rodríguez, A., Safi, K., Brown, J.C.S., Graham, L., Dunbar, R.B., Mucciarone, D.A., Magozzi, S., Somes, C., Trueman, C.N., 2021. Isoscape Models of the Southern Ocean: Predicting Spatial and Temporal Variability in Carbon and Nitrogen Isotope Compositions of Particulate Organic Matter. Global Biogeochemical Cycles 35. https://doi.org/10.1029/2020GB006901

Stowasser, G., Atkinson, A., McGill, R.A.R., Phillips, R.A., Collins, M.A., Pond, D.W., 2012. Food web dynamics in the Scotia Sea in summer: A stable isotope study. Deep-Sea Research Part II: Topical Studies in Oceanography 59–60, 208–221. https://doi.org/10.1016/j.dsr2.2011.08.004

Sutherland, K.R., Madin, L.P., Stocker, R., 2010. Filtration of submicrometer particles by pelagic tunicates. Proceedings of the National Academy of Sciences of the United States of America 107, 15129–15134. https://doi.org/10.1073/pnas.1003599107

Sweeting, C.J., Jennings, S., Polunin, N.V.C., 2005. Variance in isotopic signatures as a descriptor of tissue turnover and degree of omnivory. Functional Ecology 19, 777–784. https://doi.org/10.1111/j.1365-2435.2005.01019.x

Thorpe, S.A. (Ed.), 2009. Ocean currents: a derivative of Encyclopedia of ocean sciences, 2nd edition. Elsevier, Academic Press, Boston Heidelberg London.

Tieszen, L.L., Boutton, T.W., Tesdahl, K.G., Slade, N.A., 1983. Fractionation and turnover of stable carbon isotopes in animal tissues: Implications for ?13C analysis of diet. Oecologia 57, 32–37. https://doi.org/10.1007/BF00379558

von Harbou, L., Dubischar, C.D., Pakhomov, E.A., Hunt, B.P.V., Hagen, W., Bathmann, U. V., 2011. Salps in the Lazarev Sea, Southern Ocean: I. Feeding dynamics. Marine Biology 158, 2009–2026. https://doi.org/10.1007/s00227-011-1709-4

Wickham, H., 2016. ggplot2: Elegant Graphics for Data Analysis. Springer-Verlag, New York.

Winter, A., 2021a. 2021 1st Season Stock Assessment Falkland calamari (*Doryteuthis gahi*). Falkland Islands Fisheries Department, Stanley, Falkland Islands.

Winter, A., 2021b. 2021 2nd Season Stock Assessment Falkland calamari (Doryteuthis gahi). Falkland Islands Fisheries Department, Stanley, Falkland Islands.

Wood, S.N., 2017. Generalized Additive Models: An Introduction with R (2nd edition), 2nd ed. Chapman and Hall.

Zuur, A.F., Ieno, E.N., Walker, N., Saveliev, A.A., Smith, G.M., 2009. Mixed effects models and extensions in ecology with R, Statistics for Biology and Health. Springer New York, New York, NY. https://doi.org/10.1007/978-0-387-87458-6

Supplementary Material

Table S1 is part of the model selection process, comparing the models with an interaction and without interaction based on their AIC.

Table S1. AIC values and model comparison of $\delta^{15}N$ and $\delta^{13}C$ values (‰) for each tissue type (muscle and gladius); df = degrees of freedom and AIC for model without interaction and with interaction expresses as a tensor product

		Model	**df**	**AIC**
$\delta^{15}N$	Muscle	without interaction	6	664
		with tensor	8	667
	Gladius	without interaction	6	382
		with tensor	8	377
$\delta^{13}C$	Muscle	without interaction	6	484
		with tensor	8	456
	Gladius	without interaction	6	272
		with tensor	8	258

Table S2 is showing all niche overlap contrasts based on the Bayesian model with a 95% alpha probability.

Table S2. Niche overlap contrasts based on the Bayesian model with a 95% alpha probability for gladius and muscle tissue.

				Prob. 95%	**Prob. 95%**
Contrast	Contrast size	Group	Group size	Gladius	Muscle
ASC	large	ASC	medium	90.61	51.04
ASC	large	ASC	small	56.15	36.77
ASC	medium	ASC	large	17.06	16.32
ASC	medium	ASC	small	61.71	78.06
ASC	small	ASC	large	15.76	18.46
ASC	small	ASC	medium	90.33	88.52
ASC	large	SSC	large	72.01	35.01
ASC	large	SSC	medium	57.85	27.59
ASC	large	SSC	small	12.35	47.26
ASC	medium	SSC	large	20.83	28.89
ASC	medium	SSC	medium	33.97	26.78
ASC	medium	SSC	small	42.57	84.82
ASC	small	SSC	large	13.25	40.08
ASC	small	SSC	medium	22.63	35.27
ASC	small	SSC	small	39.56	90.5
SSC	large	ASC	large	22.07	22.08
SSC	large	ASC	medium	65.52	25.82
SSC	large	ASC	small	23.39	27.3
SSC	medium	ASC	large	9.94	14.21
SSC	medium	ASC	medium	75.03	32.65
SSC	medium	ASC	small	23.25	25.8
SSC	small	ASC	large	2.73	10.29
SSC	small	ASC	medium	71.37	49.33
SSC	small	ASC	small	22.48	39.27
SSC	large	SSC	medium	74.47	80.53
SSC	large	SSC	small	55.97	82.06
SSC	medium	SSC	large	63.51	92.58
SSC	medium	SSC	small	77.61	95.77
SSC	small	SSC	large	45.47	68.05
SSC	small	SSC	medium	73.87	69.41

Table S3. Values of $\delta^{15}N$ (‰) and estimated trophic level of Cephalopod and Crustacean species from the literature. SD = standard deviation

Genus	Species	$\delta^{15}N$		SD	Trophic Level	Reference
Cephalopods						
Doryteuthis	*gahi* (maturing)	13.18	±	0.80	5.05	Rosas-Luis *et al.* 2016
Doryteuthis	*gahi* (mature)	12.69	±	0.52	4.93	Rosas-Luis *et al.* 2016
Illex	*argentinus*	11.98	±	0.97	4.68	Rosas-Luis *et al.* 2016
Onykia	*ingens*	11.48	±	1.19	4.52	Rosas-Luis *et al.* 2016
Architeuthis	*dux*	11.6	±	1.3	4.6	Cherel *et al.* 2008
Mesonichoteuthis	*hamiltoni*	16.3	±	0.8	6.1	Cherel *et al.* 2008
Martialia	*hyadesi*	7.7	±	0.6	3.4	Cherel *et al.* 2008
Kondakovia	*longimana*	9.2	±	1.1	3.8	Cherel *et al.* 2008
Gonatus	*antarcticus*	13.3	±	0.5	5.2	Cherel *et al.* 2008
Mastigoteuthis	*psychrophila*	12.8	±	0.6	5	Cherel *et al.* 2008
Galiteuthis	*glacialis*	8.7	±	0.1	3.7	Stowasser *et al.* 2012
Crustaceans						
Euphausiids						
Euphausia	*vallentini*	5.4	±	0.8	2.6	Cherel *et al.* 2008
Euphausia	*vallentini*	14.58	±	1.16	2.8	Castro *et al.* 2021
Euphausia	*superba*	4.3	±	1.0	2.5±04	Stowasser *et al.* 2012
Thysanoessa	*spp.*	6.6	±	0.7	3.1±0.2	Stowasser *et al.* 2012
Euphausia	*frigida*	5.7	±	0.9	3±0.2	Stowasser *et al.* 2012
Euphausia	*triacantha*	7.2	±	0.9	3.3±0.3	Stowasser *et al.* 2012
Munida						
Munida	*gregaria* (pelagic larvae)	12.43	±	0.74	2.1	Castro *et al.* 2021
Munida	*gregaria* (unknown stage)	11.83	±	0.75	4.63	Rosas-Luis *et al.* 2016